# New Bioanodes: Truncated Hydride Carrier Coenzymes and Electrochemistry

Evelyne Simon and Philip N. Bartlett
Department of Chemistry
University of Southampton
Highfield
Southampton SO17 1BJ, UK
Phone: +44 23 80 59 2373 Fax: +44 23 80 59 3781 email: pnb@soton.ac.uk

Award#: N00014-98-0898





This research was sponsored by the Office of Naval Research (ONR Grant Number: N00014-98-0898; PR Number: 98PR098127-00)

# REPORT DOCUMENTATION PAGE

Form Approved OMB No. 0704-0188



| 1. AGENCY USE ONLY (Leave blank) | 2. REPORT DATE | 3. REPORT TYPE AND DATES COVERED |
|---|---|---|
| | 1998 | Project Report |

4. TITLE AND SUBTITLE

New Bioanodes: Truncated Hydride Carrier Coenzymes and Electrochemistry

5. FUNDING NUMBERS

N00014-98-0898

6. AUTHOR(S)

Evelyne Simon and Philip N. Bartlett

7. PERFORMING ORGANIZATION NAME(S) AND ADDRESS(ES)

University of Southampton, Highfield, Department of Chemistry, Southampton, SO17 1BJ, United Kingdom

8. Performing Organization Report Number

9. SPONSORING/MONITORING AGENCY NAME(S) AND ADDRESS(ES

Office of Naval Research, European Office, PSC 802 Box 39, FPO AE 09499-0039

10. SPONSORING/MONITORING AGENCY REPORT NUMBER

98PR098127-00

11. SUPPLEMENTARY NOTES

This research was sponsored by the Office of Naval Research (ONR Grant Number: N00014-98-0898; PR Number: 98PR098127-00). Reproduction in whole or in part is permitted for any purpose of the United States Government. 66 pages

12a. DISTRIBUTION/AVAILABILITY STATEMENT

Approved for public release; distribution is unlimited.

12b. DISTRIBUTION CODE

A

ABSTRACT (Maximum 200 words)

The long term goal of the project was to develop novel biofuel cells suitable for energy harvesting and low level power generation. The original objectives in collaboration with Cass (Imperial College, UK), Ellington (Texas) and Bugg (Warwick University, UK) were to develop synthetic, cost effective and more stable analogues of NADH which can be used in conjunction with a protein-engineered dehydrogenase enzyme to provide the electrochemical basis of a novel bioanode for use in a biofuel cell.

It was planned to synthesis a series of NADH analogues of increasing complexity (Bugg) and then to use this series of analogues, in conjunction with protein evolution studies, to develop engineered dehydrogenase enzymes which are capable of utilizing these molecules in place of NADH (Cass and Ellington). The mechanism of the electrochemical oxidation of these NADH analogues at chemically modified electrodes was to be studied and efficient electrodes developed for use in conjunction with the modified enzymes as the anode of a biofuel cell. Methods for the immobilization of the NADH analogues onto electrode surfaces and the resulting electrochemistry of the immobilized molecules were also to be studied.

14. SUBJECT TERMS

ONR, Biofuel cells, Analogues, Dehydrogenase enzyme, Bioanode, Electrochemical oxidation, Electrodes NADH oxidation, Electrochemical behavior

15. NUMBER OF PAGES

16. PRICE CODE

| 17. SECURITY CLASSIFICATION OF REPORT | 18. SECURITY CLASSIFICATION OF THIS PAGE | 19, SECURITY CLASSIFICATION OF ABSTRACT | 20. LIMITATION OF ABSTRACT |
|---|---|---|---|
| UNCLASSIFIED | UNCLASSIFIED | UNCLASSIFIED | UL |

**CONTENTS:**

# The scope of the project

The long term goal of the project was to develop novel biofuel cells suitable for energy harvesting and low level power generation.

Our original objectives, in collaboration with Cass (Imperial College, UK), Ellington (Texas) and Bugg (Warwick University, UK) were to develop synthetic, cost effective and more stable analogues of NADH which can be used in conjunction with a protein-engineered dehydrogenase enzyme to provide the electrochemical basis of a novel bioanode for use in a biofuel cell.

It was planned to synthesis a series of NADH analogues of increasing complexity (Bugg) and then to use this series of analogues, in conjunction with protein evolution studies, to develop engineered dehydrogenase enzymes which are capable of utilising these molecules in place of NADH (Cass and Ellington). The mechanism of the electrochemical oxidation of these NADH analogues at chemically modified electrodes was to be studied and efficient electrodes developed for use in conjunction with the modified enzymes as the anode of a biofuel cell. Methods for the immobilisation of the NADH analogues onto electrode surfaces and the resulting electrochemistry of the immobilised molecules were also to be studied.

# Work completed in Southampton

## 1. Catalysts for NADH oxidation

The oxidation of NADH at bare electrodes requires a high overpotential (~1V) and leads to fouling of the electrode surface by reaction products. A mediator is necessary to perform the reaction at lower overpotential.

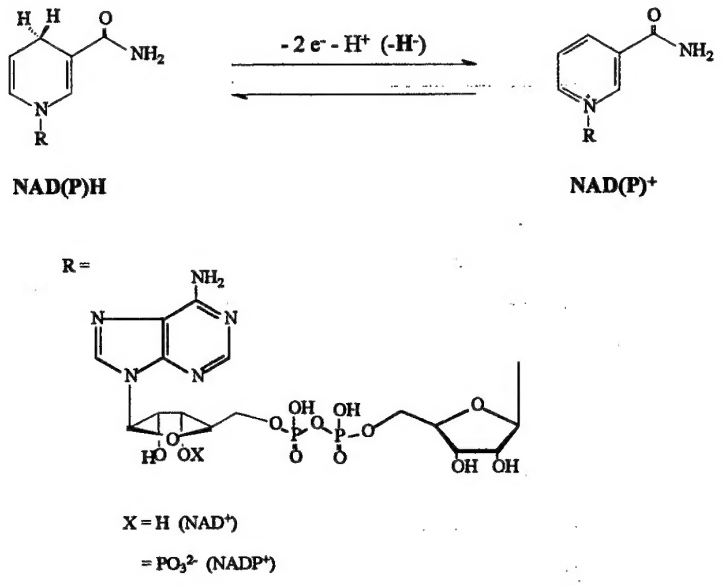


**Figure 1: NADH oxidation.**

The use of modified electrodes is one way to overcome the problem of the electrode poisoning. The mediator can be deposited as a film on the electrode surface and thus shuttles the electrons from the electrode to the NADH and prevents the adsorption of reaction products onto the electrode surface, whilst reducing the overpotential for the reaction.

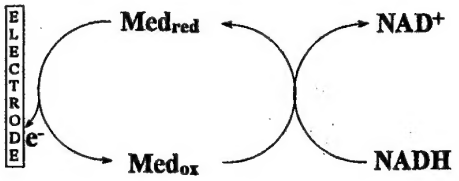


**Figure 2: Modified electrode for the oxidation of NADH.**

Many mediators for NADH oxidation have been studied [1, 2]. It has been found that in most cases the structures of the mediators have the features shown in Figure 3a.

Poly(aniline), a conducting polymer, also has these structural features and can be used as a catalyst for NADH oxidation (Figure 3b).

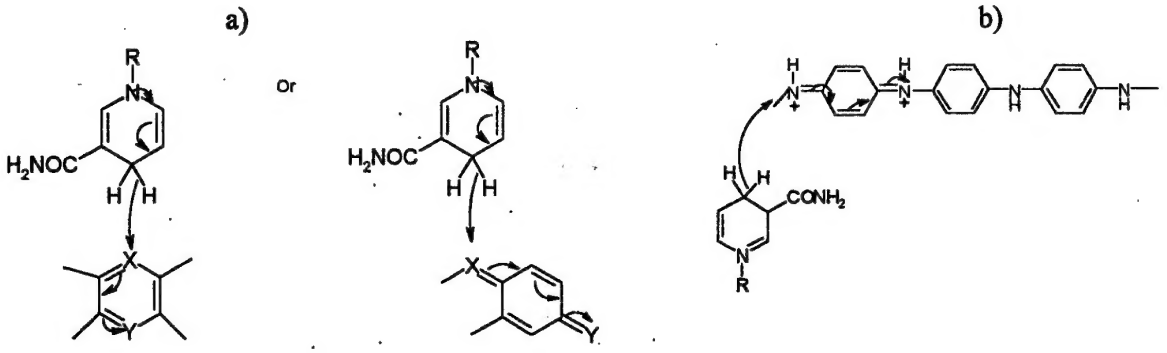


**Figure 3: a) Structures of mediators for NADH oxidation. b) poly(aniline) [emeraldine form] as a mediator for NADH oxidation.**

Poly(aniline) exists in three different redox states: leucoemeraldine, the fully reduced state, emeraldine, the semi-oxidised state, and pernigraniline, the fully oxidised state (see Figure 4). Only the protonated emeraldine form is conducting, but it is rapidly deprotonated at pH above 5.

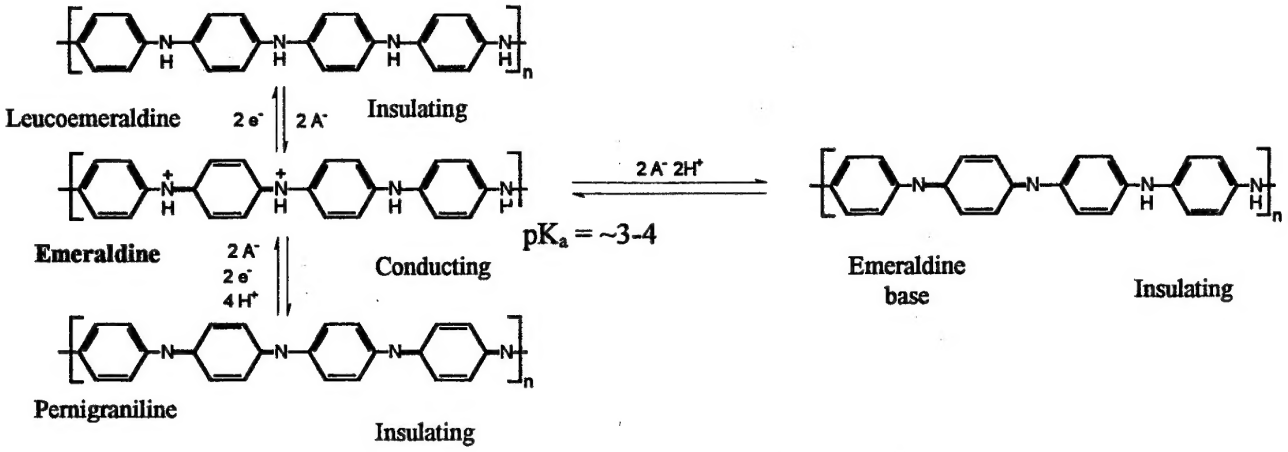


**Figure 4: Redox states of poly(aniline).**

NADH is quickly hydrolysed at pH lower than 7 and the emeraldine state of poly(aniline) is deprotonated at pH above 5. Therefore it is necessary to modify the poly(aniline) so it remains protonated, and thus conducting, at pH 7 and can be used as a mediator for NADH

oxidation. Anions can be introduced on the poly(aniline) backbone by co-polymerising aniline with a substituted aniline containing a carboxylic or a sulfonic acid group to obtain a self-doped poly(aniline). Another way to maintain the emeraldine conductivity at pH 7 is to dope the poly(aniline) with large poly(anions) such as Nafion®, poly(acrylate) or poly(vinylsulfonate).

Within this project we have investigated all of these different ways to maintain the conductivity of the emeraldine form at pH 7.

## 1.1 Self-doped poly(aniline) films

Self-doped poly(aniline) films (Figure 5) have been studied.

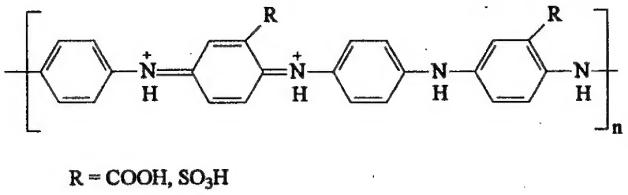


**Figure 5: Self-doped poly(aniline).**

Aniline was electropolymerised in the presence of 2- or 3-substituted anilines (such as anthranilic acid and metanilic acid). Some of the resulting copolymers are electroactive and conducting at pH 7, and catalyse NADH oxidation.

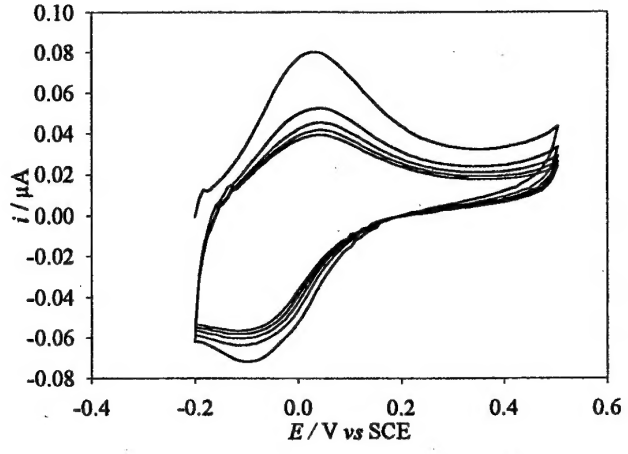


**Figure 6: Electrochemical behaviour of a copolymer of aniline and anthranilic acid (1:1 ratio) in 0.1 M citrate/phosphate buffer pH 7, $v$= 50 mV $s^{-1}$ (electropolymerisation by CV at 60 °C, $Q_{growth}$= 51.34 mC).**

In figure 7, the catalytic currents for NADH oxidation observed at a poly(aniline-anthranilic acid) modified electrode are plotted against NADH concentration. Thicker films seem to give higher currents. Nonetheless, the results for three films of about the same thickness (92, 93, 95 mC) gave different results.

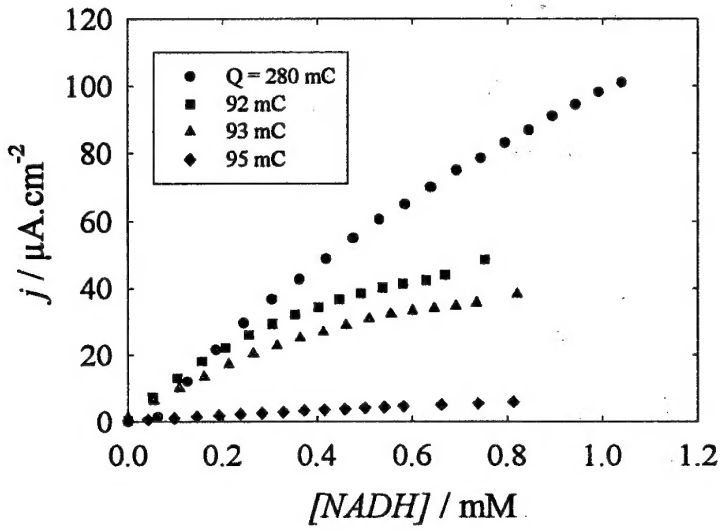


**Figure 7: Catalytic currents for NADH oxidation at 0.05 V vs SCE at an anthranilic acid and aniline copolymer modified electrode (deposition charge = 51 mC at 60 °C, geometric area = 0.38 $cm^2$). 0.1 M citrate-phosphate buffer pH 7.0, 25 °C, $W$ = 9Hz.**

The lack of reproducibility of the electropolymerisation of such copolymers is probably the reason for the difference in the catalytic currents observed. Note that the current densities for NADH oxidation recorded for these films are similar to those reported below for the PANi composite films. Similar problems were encountered for other copolymer films.
Due to this problem of reproducibility, these copolymers were not used further in this study.

## 1.2 Poly(aniline)-poly(anion) composite films

### *1.2.1 Poly(aniline)-Nafion®*

Composite materials have properties which differ from those of their individual components. Conducting polymers, like poly(pyrrole), are brittle and present poor mechanical properties. But these properties can be modified by depositing the polymers in

a material like poly(vinyl chloride). Poly(pyrrole)/PVC composite membranes present the conductivity of poly(pyrrole) combined with the mechanical properties of PVC. Nevertheless electropolymerisation of pyrrole in PVC is slow, this polymer is not porous and it is not ionically conductive. It is actually more interesting for our purposes to have a host material which is chemically inert, porous, mechanically stable and ionically conductive. Nafion® (Figure 8), a perfluorosulfonate ionomer from Du Pont, presents these properties.

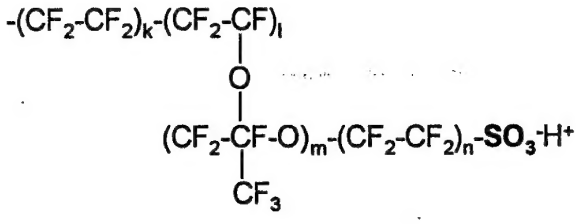


**Figure 8: Structure of Nafion®.**

Nafion® can be used to impregnate inert membranes (Gore-Tex membranes), as a membrane, or as a film cast on the electrode. Poly(pyrrole) has been electropolymerised in impregnated membranes or in Nafion® cast films (but not in Nafion® membranes, because of their low porosity) [3].

It has been shown that the sulfonate groups in Nafion® are incorporated as charge compensators in poly(pyrrole) [4, 5] and poly(aniline) [4]. During the polymer redox process the cation movement is enhanced and anion movement is hindered. Thus the composite film acts as a cation exchanger.

It has been shown in our group that PANi doped with poly(anion)s such as poly(vinylsulfonate) (PVS) or poly(styrenesulfonate) (PSS) is conductive in neutral aqueous media and catalyses NADH oxidation [6, 7]. Since we are looking at doping poly(aniline) with other poly(anion)s, Nafion® appears to be an interesting dopant. Poly(aniline) has been deposited on precast Nafion® films [4, 8, 9], and the composite films were electroactive at pH>5. An amperometric urea biosensor based on a PANi-Nafion composite electrode has been prepared [9]: PANi was electropolymerised on an electrode coated with a Nafion® film, urease was then cross-linked (using glutaraldehyde solution as the cross-linking agent) to the composite to form the biosensor. This method of immobilisation of the enzyme may be used in our work to prepare a bioanode.

To prepare PANi-Nafion® composite film, two different methods were used:

- electropolymerisation of aniline within a Nafion® precast film,
- electropolymerisation of aniline from a solution containing Nafion®.

a- Nafion® precast film

A glassy carbon electrode was first coated with a Nafion® film, then the poly(aniline) was electropolymerised from a solution of aniline in acid by cyclic voltammetry.

A green film was observed on the electrode surface, the modified electrode was transferred to a 1.0 M HCl solution and the voltammogram was recorded (Figure 9). The electrochemical behaviour of the PANi-Nafion® composite film is comparable to that of PANi-HCl : two redox systems corresponding to the oxidation of the leucoemeraldine to emeraldine (at ~0.2 V) and to the oxidation of the emeraldine to pernigraniline (at ~0.8 V), are observed.

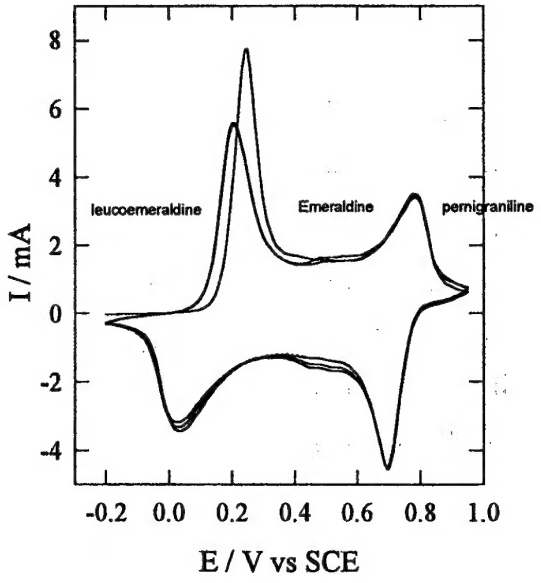


**Figure 9: Electrochemical behaviour of a PANi-Nafion® composite film in 1.0 M HCl ($Q_{growth}$= 150 mC, rea = 0.38 cm$^2$), $v$ = 50 mV.s$^{-1}$.**

The electrode was rinsed with water and then transferred to 0.1 M citrate-phosphate buffer solution containing 0.5 M $Na_2SO_4$ solution. The polymer presents one redox system, the two systems observed in acidic media are superimposed - the system emeraldine/pernigraniline is shifted to lower potential when the pH is increased. Then the electrode was transferred to a citrate/phosphate buffer solution at pH 7, the signal was stable after a few cycles (about 5) (Fgure 10).

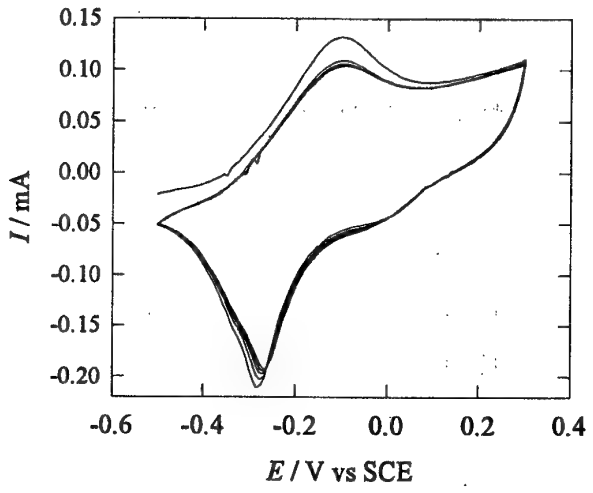


**Figure 10: Electrochemical behaviour of a PANi-Nafion® composite film in 0.1 M citrate/phosphate buffer pH = 7 ($Q_{growth}$ = 150 mC, area = 0.38 $cm^2$), $v$ = 50 mV $s^{-1}$.**

Some NADH (1 mM) was then added in the electrochemical cell, but no catalysis was observed. After these experiments at pH 7, the film was still green.

Ascorbate oxidation at this modified electrode was also tested. But, again no catalytic current was observed when ascorbate was added to the cell.

To see if the film is permeable, a voltammogram of a solution of ferricyanide in 0.1 M $KNO_3$ was recorded : no redox reaction was observed. Thus it appears that this composite film is not permeable to solution species. The poly(aniline) film probably grows beneath the Nafion® film and this film prevents species from the solution (NADH, ascorbate or ferricyanide) reaching the PANi film.

A thicker poly(aniline) film (266 mC) deposited on a Nafion® film (0.2 µm), was not electroactive at pH 7. in this case the poly(aniline) probably grew through and then outside

the Nafion film and was then deprotonated when in contact with the buffer solution at pH 7 giving an insulating outer polymer layer.

Further films were prepared in which the amount of PANi deposited (calculated from data in the literature [10]) was less than the Nafion® film (it is assumed that the density of the Nafion® film is 1.98 $g.cm^{-3}$ [11]) or about the same thickness.

In all the cases, no catalysis of the oxidation of NADH or ascorbate was observed, and none of the films are permeable to ferricyanide.

It is important to note that the currents observed are much smaller (~ 30 times) than the currents observed with poly(aniline)-poly(vinylsulfonate) composite electrode.

The PANi-Nafion® composite films are probably impermeable to anions and permeable to cations, the composite film being a cation exchanger. Some cations have been detected at PANi-Nafion® composite electrodes [12].

This method of doping the poly(aniline) with poly(anion) is not suitable for the oxidation of NADH (which is negatively charged). To form composites of poly(aniline)-poly(anion), it will be necessary to introduce the poly(anion) into the electropolymerisation solution and thus perform a co-immobilisation of PANi and the poly(anion) which will be entrapped in the PANi network as it grows.

Since the commercial solution of Nafion® is acidic, we tried to electropolymerise aniline directly from that solution following a method that has already been described [13]. However all attempts to obtain polymer films by galvanostatic deposition or cyclic voltammetry failed. Polymers were formed but they did not adhere to the electrode surface.

Since this method of forming a PANi-Nafion® composite failed, the Nafion® was dissolved in the electropolymerisation solution and co-immobilised with PANi on the surface of a glassy carbon electrode.

b- Nafion® dissolved in the electropolymerisation solution

The commercial solution of Nafion® contains alcohols and water (5 wt.%). This solution cannot be diluted with an aqueous or a methanolic solution of HCl or $H_2SO_4$, due to precipitation of the ionomer. To dissolve the Nafion®, it is necessary to first dilute the

commercial solution with methanol and then to add slowly the aniline dissolved in 1.0 M HCl. The electropolymerisation can then be performed by cyclic voltammetry.

The rate of polymerisation is much slower than in a growth solution containing poly(vinylsulfonate). The film obtained is light green.

The modified electrode was transferred to a fresh solution of 1 M HCl, the voltammetry recorded between –0.2 to 0.9 V shows 2 redox systems, as is usual for PANi-modified electrodes in acidic media (Figure 11).

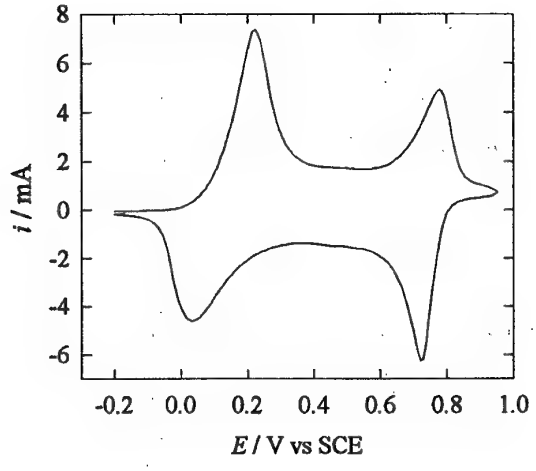


**Figure 11: PANi-Nafion® film deposited from a solution containing 1.0 M HCl, MeOH and Nafion®. Deposition charge = 158 mC (area = 0.38 $cm^2$), 1.0 M HCl, $\nu$=50 mV $s^{-1}$**

After washing the electrode with water, it was placed in a cell containing 0.1 M citrate/phosphate buffer at pH 7. A voltammogram was recorded and then 1 mM of ascorbate was added to the cell: catalysis of ascorbate oxidation was observed (Figure 12).

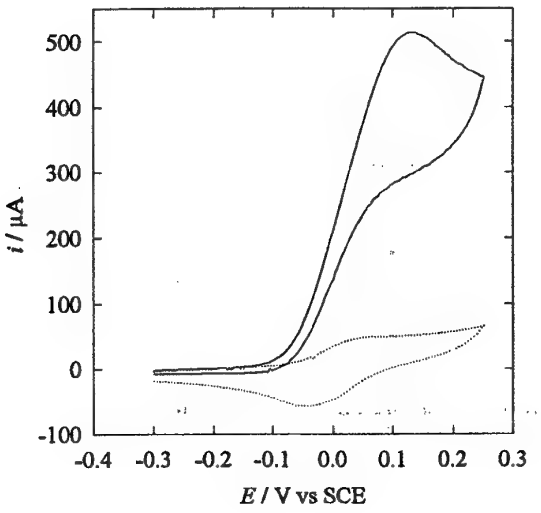


**Figure 12: Catalysis of ascorbate oxidation at PANi-Nafion® composite film in 0.1 M citrate-phosphate buffer pH 7.0, $\nu = 50$ mV $s^{-1}$. (————) without ascorbate; (————) with 1mM ascorbate**

The catalysis of ascorbate oxidation was then performed at a rotating disc electrode coated with this PANi-Nafion® composite electrode. The electrode was rotated at 5 Hz and the potential swept from -0.2 to 0.2 V (Figure 13).

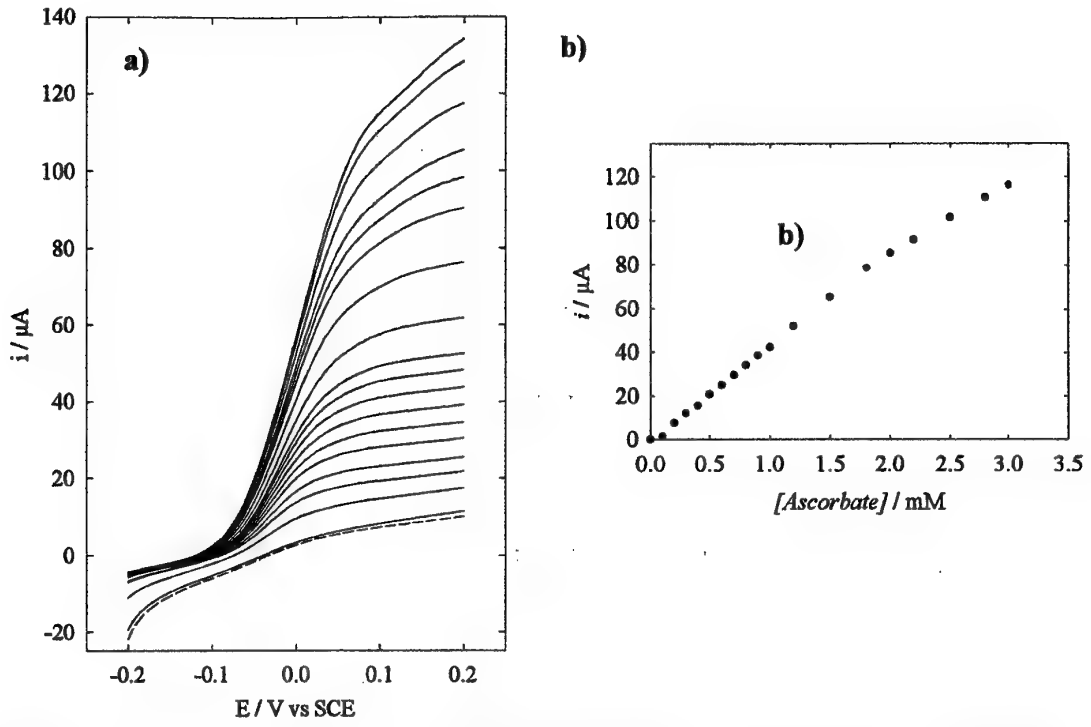


**Figure 13: a) Ascorbate oxidation at a PANi-Nafion modified electrode, in 0.1M citrate/phosphate buffer pH 7.0, 25 °C, under argon, $W = 5$ Hz, potential swept from -0.2 to +0.2 V vs SCE at 2 mV $s^{-1}$ b) Plot of the plateau current versus the concentration of ascobate in the bulk of the solution.**

Nonetheless, despite the evident catalysis at the PANi-Nafion® composite it is important to note that PANi-PVS composite films give catalytic currents about 5 times higher for ascorbate oxidation, [14].

Although the PANi-Nafion® composite film presents a very stable system under cyclic voltammetry at pH 7.0, it does not show any catalytic activity towards NADH oxidation. Consequently, this composite was not used in the rest of our project.

### *1.2.2 Poly(aniline)-poly(acrylate) composite films*

Poly(aniline) composite films, Figure 14, have been used for the oxidation of NADH [6, 7, 15].

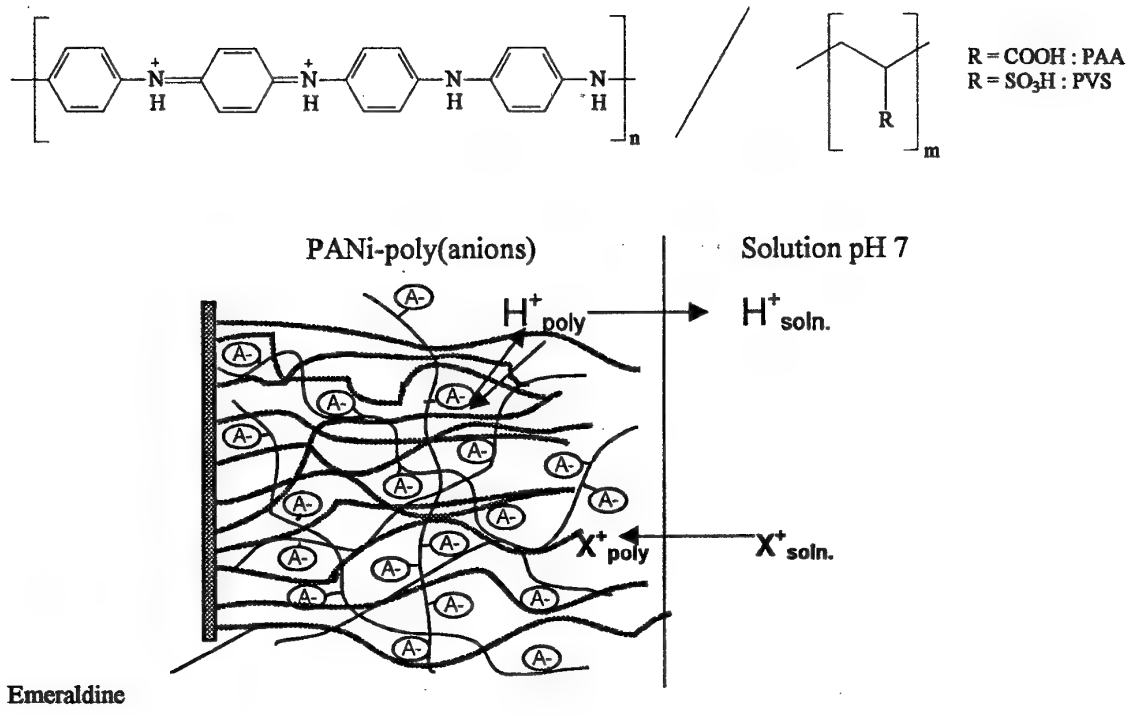


**Figure 14: Poly(aniline)-poly(anions) composite films.**

The poly(anions) are co-immobilised with poly(aniline) during the aniline electropolymerisation process. The presence of poly(anion) in the poly(aniline) film changes its properties. At pH 7, protons tend to migrate from the film to the solution, as the counter-ions of PANi are immobilised in the polymer matrix, cations have to enter the polymer to ensure electroneutrality (Figure 14). As protons are mobile, we hope to preserve the protonation of the composite film at pH 7 as the cation movement will be hindered.

The poly(aniline)-poly(acrylate) [PANi-PAA] composite films were electrodeposited from an aniline solution containing 15% of poly(acrylate) in 2.7 M HCl, by cyclic voltammetry onto a glassy carbon electrode (Figure 15 a). The electrode potential was swept from -0.2

to 0.9 V vs SCE at 50 mV $s^{-1}$ for the first cycle, a nucleation loop is observed due to the formation of anilinium radicals. For the subsequent cycles, the potential is swept from -0.2 to 0.78 V to avoid degradation of the poly(aniline) due to nucleophilic attack by water resulting in the formation of quinone moieties which terminates the electropolymerisation process. A composite poly(aniline) film coats the electrode, this film is porous as shown on Figure 15 b.

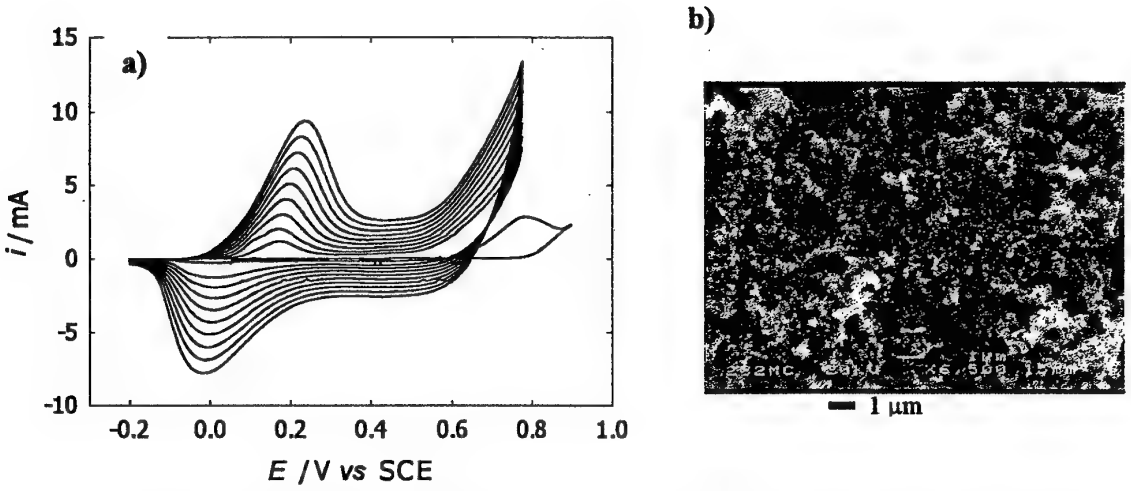


**Figure 15: a) Electropolymerisation by cyclic voltammetry of aniline on a glassy carbon disc electrode (area = 0.38 $cm^2$) in 2.7 M HCl in the presence of 15% poly(acrylic acid). During the first cycle the potential is swept from -0.2 to 0.9 V vs SCE at 50 mV $s^{-1}$ and then for all the subsequent cycles it is swept from -0.2 to 0.78 V. b) Scanning Electron Microscope image of a poly(aniline)-poly(acrylic) composite film deposited on a glassy carbon electrode (scale bar 1 μm).**

The PANi-PAA film shows two redox systems at pH 1.0 corresponding to the oxidation of leucoemeraldine in emeraldine at 0.23 V vs SCE and the oxidation of emeraldine to pernigraniline at 0.78 V (Figure 16a).

The two redox systems, clearly distinct at pH 1, shift with increasing pH and eventually merge into one broad system at pH > 5. The electrochemical behaviour of a PANi-PAA modified electrode at pH 7.0 is shown in Figure 16b.

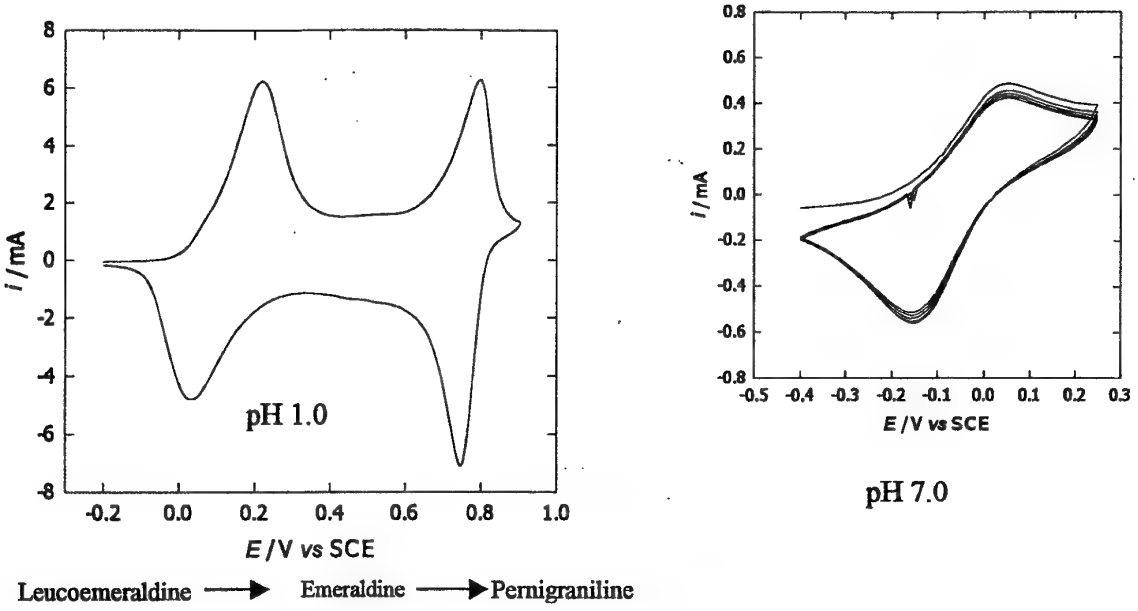


**Figure 16: a) Electrochemical behaviour of a PANi-PAA modified electrode in 0.1M HCl-KCl at pH 1.0, $\nu$ = 20 mV $s^{-1}$. The film was grown with a deposition charge of 150 mC on an 0.38 $cm^2$ electrode. b) Electrochemical behaviour of the same PANi-PAA modified electrode in 0.1M citrate-phosphate buffer at pH 7.0, $\nu$= 20 mV $s^{-1}$.**

It was observed for thin PANi-PAA films, that about 9% of the charge for cycling in acid was lost on cycling from –0.2 to 0.4 V at pH 7 and thereafter the charge stabilises. For thicker films no charge loss was observed after the first cycle at pH 7, but some loss was observed after several cycles at pH 7.

The conductivity of the PANi-PAA film was studied using a dual microband electrode. A film was electropolymerised across the 20 μm gap between the two microband electrodes and the resistance across the film was measured as a function of the potential of the film [6]. The plot of log $R$ against the film potential shows that the minimum resistance of the film in pH 7.0 solution occurs at -30 mV (Figure 17). This value is similar to the values found for poly(aniline)-poly(vinylsulfonate) (-50 mV) and poly(aniline)-poly(styrenesulfonate) (-25 mV) films [6, 7].

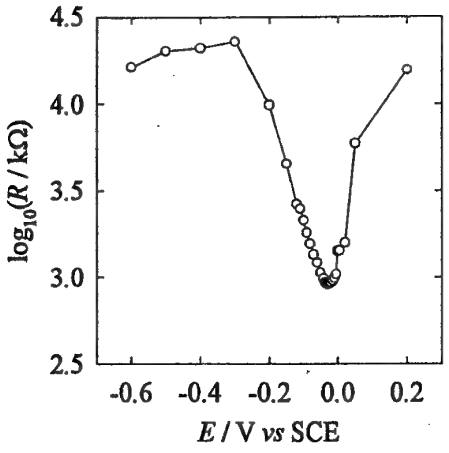


**Figure 17: Logarithm of the resistance of PANi-PAA composite film deposited across the gap (20 µm) between two screen printed carbon microband electrodes, measured in 0.1M citrate-phosphate buffer at pH 7.0.**

The protonation of the poly(aniline) film can be studied by UV-visible spectroscopy. According to the literature [16], the protonated emeraldine form of poly(aniline) has an absorption peak at 340 nm corresponding to the $\pi$-$\pi^*$ transition of the benzene rings, a broad absorption peak at 440 nm corresponding to the radical cation (semiquinone structures) and a very broad band at 750 nm due to imine moieties (quinone structures). In neutral solution the emeraldine is deprotonated and consequently not conducting, and the adsorptions at 440 and 750 nm disappear. Chemically prepared PANi-PAA composites have been shown to give similar UV-vis spectra [17].

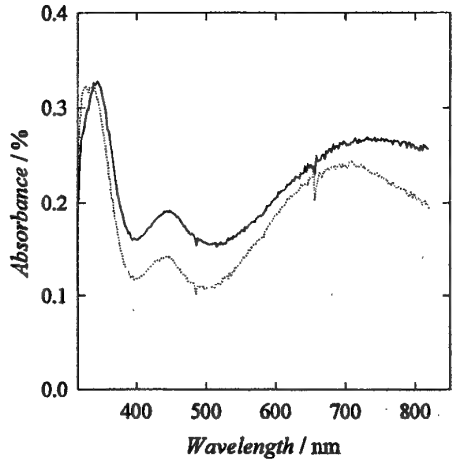


**Figure 18: UV-vis spectra of a PANi-PAA film deposited (3 mC cm$^{-2}$) onto an ITO-glass electrode. (———) : PANi-PAA film held at +0.5 V vs SCE in 1.0 M HCl, then dried at 40 °C. (———) : PANi-PAA immersed in 0.1 M citrate-phosphate buffer pH 7.0.**

The PANi-PAA films were deposited on an ITO-glass transparent electrode and the UV-vis spectra were recorded. For the acid treated film, in its emeraldine form, three bands at 340, 440 and 750 nm are present as expected (Figure 18). The same spectra were obtained with dried films or in solution. After treating the film at pH 7.0, the bands at 340 and 440 nm do not change significantly but there is a blue shift in the long-wavelength band at ~700 nm which causes the film to change in appearance from green to blue. From this experiment we can conclude that much of the PANi-PAA in the emeraldine state remains protonated at pH 7.

Since the poly(aniline)-poly(acrylate) composite film remains electroactive and conducting at pH 7, it can be used as a mediator for NADH oxidation.

The modified electrode obtained is an electrocatalytic surface for NADH oxidation at +0.05V *vs* SCE in 0.1 M citrate/phosphate buffer at pH 7. The amperometric responses of these composite poly(aniline) films for NADH oxidation have been studied in detail and fitted to a kinetic model [6, 15].

*1.2.3 Kinetic model for NADH oxidation at poly(aniline)-poly(anion) composite films*

According to our kinetic model, the oxidation of NADH at the modified electrode can be described by the following mechanism (figure 19) :

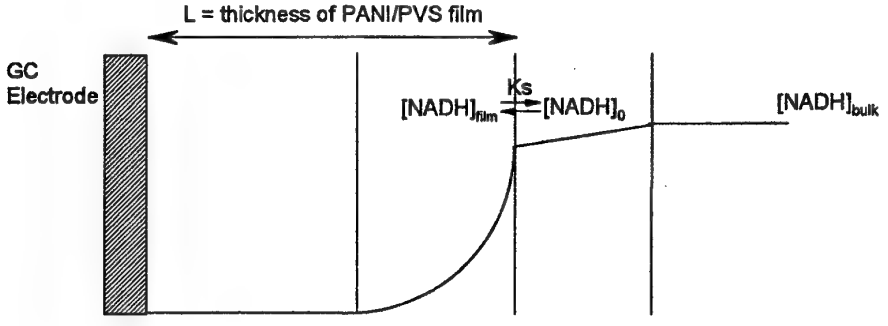


**Figure 19: Mechanism for NADH oxidation in poly(aniline) composite film.**

$$NADH_{bulk} \underset{k_{D,S}}{\overset{k_{D,S}}{\rightleftharpoons}} NADH_0$$

Solution mass transport

$NADH_0 \underset{}{\overset{K_S}{\rightleftharpoons}} NADH_{film}$ Partition into the film

$NADH_0 \underset{}{\overset{K_S}{\rightleftharpoons}} NADH_{film}$ Adsorption within the film

$\{NADH\} \xrightarrow{k_{cat}} \{NAD^+\} + H^+ + 2\,e^-$ Oxidation of bound NADH

$\{NAD^+\} \underset{}{\overset{K_i}{\rightleftharpoons}} NAD^+_{film} + \{site\}$ Desorption of product

$NAD^+_{film} \underset{}{\overset{K_P}{\rightleftharpoons}} NAD^+_0$ Partition into the film

$NAD^+_0 \underset{k'_{D,P}}{\overset{k'_{D,P}}{\rightleftharpoons}} NAD^+_{bulk}$ Solution mass transport

where the subscripts "bulk", "0" and "film" refer to the bulk solution, the interface between the polymer and the solution, and the inside of the film, respectively; $k'_{D,X}$ is the mass transport coefficient for the species X at the rotating disc electrode ($k'_{D,X} = 1.554 D_X^{2/3} \nu^{-1/6} W^{1/2}$); where $D_X$ is the diffusion coefficient, $\nu$ the kinematic viscosity and $W$ the rotation speed in Hz [18]; $K_S$ and $K_P$ are the partition coefficients for NADH and $NAD^+$ into the film respectively; $K_M$ is the equilibrium constant for adsorption and $k_{cat}$ the rate constant for oxidation of the adsorbed NADH; site represents a catalytic site within the film; and $K_i$ is the inhibitor constant for reversible inhibition by $NAD^+$. According to this mechanism the current for NADH oxidation is given by [3]

$$i = nFAK_M D_{S,film} y / L \qquad (1)$$

with

$$y = \left\{2\varepsilon\left[\alpha - \ln(1+\alpha)\right]\right\}^{1/2} \tanh\left[\frac{\varepsilon^{1/2}\alpha}{(1+\alpha)\left\{2\left[\alpha - \ln(1+\alpha)\right]\right\}^{1/2}}\right] \quad (2)$$

$$\varepsilon = \frac{L^2[\text{site}]k_{\text{cat}}}{D_{\text{S,film}}K_{\text{M}}} \quad (3)$$

and

$$\alpha = K_{\text{S}}[\text{NADH}_0]/K_{\text{M}} \quad (4)$$

where $L$ is the film thickness and [site] is the concentration of active catalytic sites within the film. Assuming that the film thickness is linearly related to the charge passed during the film growth process, $Q_{\text{deposition}}$,

$$L = \sigma_{\text{deposition}} Q_{\text{deposition}} \quad (5)$$

where $\sigma_{\text{deposition}}$ is a constant.

In these equations $[\text{NADH}]_0$ refers to the concentration of the NADH at the outside of the polymer film. For the rotating disc electrode this concentration is related to the bulk concentration by

$$[\text{NADH}_0] = [\text{NADH}_{\text{bulk}}] - i/nFAk'_{\text{D,S}} \quad (6)$$

The effects of $NAD^+$ inhibition may be taken into account [3] by replacing $K_{\text{M}}$ and $k_{\text{cat}}$ by

$$k'_{\text{cat}} = k_{\text{cat}}/(1 - K_{\text{M}}/K_{\text{i}}) \quad (7)$$

and

$$K'_{\text{M}} = K_{\text{M}}\left\{\frac{1 + \left(K_{\text{P}}[\text{NAD}^+_0] + K_{\text{S}}[\text{NADH}_0]\right)/K_{\text{i}}}{(1 - K_{\text{M}}/K_{\text{i}})}\right\} \quad (8)$$

respectively, where

$$[\text{NAD}^+_0] = [\text{NAD}^+_{\text{bulk}}] + i/nFAk'_{\text{D,P}} \quad (9)$$

The different limiting cases and the corresponding expressions for the current for NADH oxidation arising from equation (1) are summarised in the case diagram given in figure 20. In the following analysis we shall use these expressions to fit the amperometric response of our films to NADH.

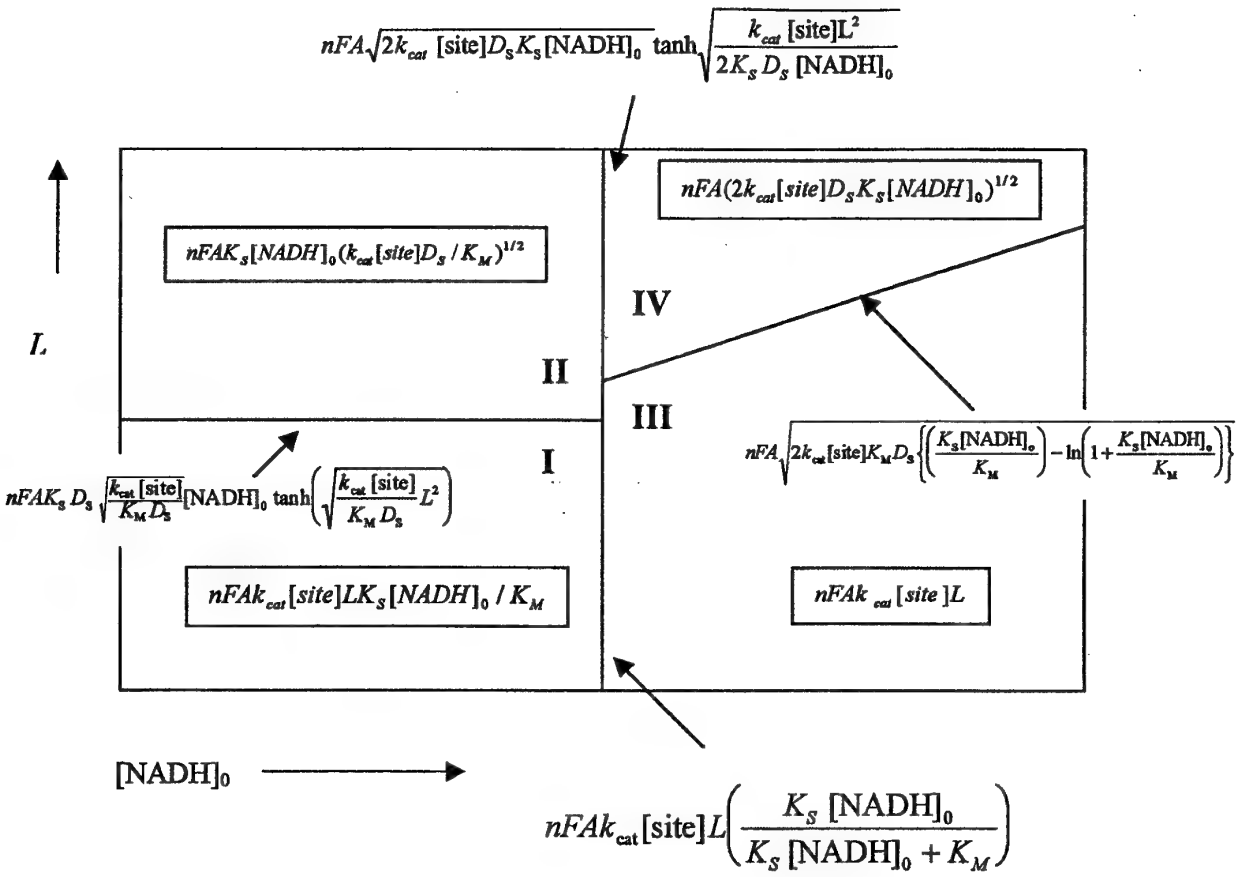


**Figure 20: Case diagram derived from eqn. (1) for the kinetic model. The different equations represent the different limiting expressions for the current in each case and across the boundaries between each pair of cases.**

In the following analysis we use these expressions to fit the amperometric response of our poly(aniline) composite films to NADH. To do this, we first identify the appropriate initial and final case for a given set of data by considering the dependence of the current on the experimental variables of NADH concentration, $[\text{NADH}]_0$, and the film thickness, $L$.

Case I corresponds to no concentration polarisation in the polymer layer. In this case diffusion within the layer is fast, therefore $NAD^+$ diffuses out of the film as soon as it is produced. Thus there is no $NAD^+$ in the layer and the concentration of NADH is uniform throughout the film. This is valid only for thin films and when the concentration of NADH is insufficient to saturate the reaction sites.

Case II corresponds to unsaturated kinetics. In this case the film is thick but the concentration of NADH is still insufficient to saturate the sites. Therefore all NADH is

consumed in a first order reaction layer (thickness $X_k$) at the outside of the film. The current will be independent of film thickness and the rate of the chemical reaction will be far greater than the rate of diffusion of NADH in the film, hence the reaction will be diffusion controlled.

Case III corresponds to saturated kinetics. The concentration of NADH is sufficient to saturate the sites and the film is thin. Thus the reaction of NADH occurs with zero order kinetics throughout the whole film. The current will be dependent on film thickness and the concentration of sites in the polymer film, but independent of NADH concentration.

Case IV describes partially saturated kinetics. The NADH concentration is sufficient to saturate the sites at the outside of the film but then falls as it is consumed within the film, so that the kinetics become unsaturated further into the film. The current is independent of film thickness and is half order with respect to concentration of sites within the film and the concentration of NADH.

The appropriate expression for the current is selected from Figure 20. The experimental data are then fitted to the appropriate expression using a commercial non-linear least squares fitting routine (SigmaPlot, Jandel Scientific).

We studied the influence of the molecular weight of poly(acrylic acid) (Figure 21). It appeared that a molecular weight of 8000 gave the highest catalytic current. Therefore PAA with a molecular weight of 8000 was used in all subsequent experiments. We also noticed that the response time for thick films (395 mC $cm^2$) to reach the steady state response was long (50 s) and much shorter (10 s) for thin film (240 mC $cm^2$). Consequently for studying the influence of the rotation speed and of the potential we used thin films.

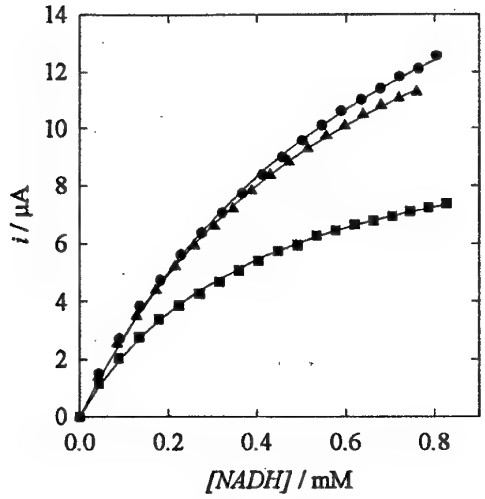


**Figure 21: Currents measured for NADH oxidation at +50 mV vs SCE at a PANi-PAA modified electrode (deposition charge 236 mC cm$^{-2}$) plotted against the NADH concentration at a rotation speed of 9 Hz, in 0.1 M citrate-phosphate buffer pH 7, under argon. Molecular weight of PAA: ■, 1200: ●, 8000 and ▲, 15 000 Da.**

The NADH oxidation at +50 mV shows reasonable reproducibility (Figure 22), although there is some scatter for [NADH] > 0.5 mM. In addition, when the same film is used for more than one experiment, a drop in the catalytic currents is observed. This decrease is consistent with the behaviour described for the cyclic voltammetry of the film.

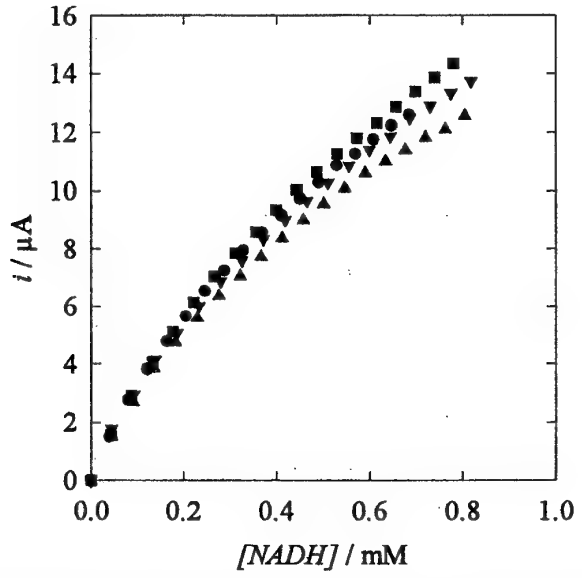


**Figure 22: Currents measured for NADH oxidation at +50 mV vs SCE at a PANi-PAA modified electrode (deposition charge 236 mC cm$^{-2}$) plotted against the NADH concentration at a rotation speed of 9 Hz, in 0.1 M citrate-phosphate buffer pH 7, under argon. Results for four replicate films prepared using 8000 Da poly(acrylate) under identical conditions.**

We also studied the influence of the potential on the catalytic current for NADH oxidation, Figure 23. The fastest responses were obtained at a potential ≤ 50mV and at higher potential the response times become very long (more than 20 min). This is consistent with the resistance measurement since at higher potential the films become less conducting and consequently charge propagation through the film is slow. The points in Figure 23 represent the experimental data and the solid lines, the currents calculated using the kinetic model for the boundary I-III. As the potential becomes more anodic, the parameter $k_{cat}[site]\sigma_{growth}$ increases and there is a corresponding slight decrease in $K_M/K_s$. The value of the rate constants obtained from the fits are given in the table.

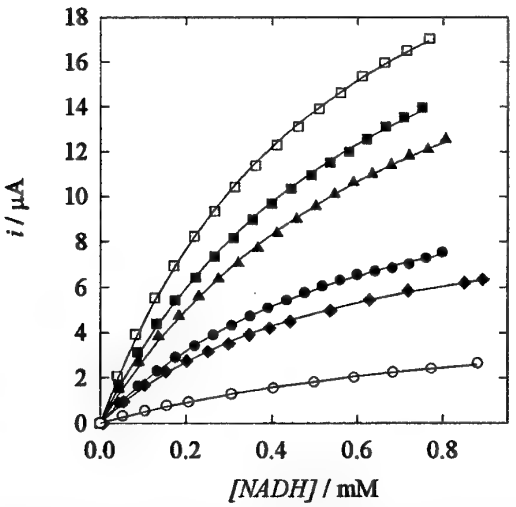


| *E vs.* SCE / V | $k_{cat}[site]\sigma$ / mol cm$^{-2}$ mC$^{-1}$ s$^{-1}$ | $K_M/K_S$ / mM |
|---|---|---|
| -0.030 | $(0.86 \pm 0.04)10^{-6}$ | $1.055 \pm 0.071$ |
| 0.000 | $(1.56 \pm 0.03)10^{-6}$ | $0.558 \pm 0.195$ |
| +0.025 | $(2.06 \pm 0.02)10^{-6}$ | $0.635 \pm 0.138$ |
| +0.050 | $(3.69 \pm 0.07)10^{-6}$ | $0.775 \pm 0.025$ |
| +0.075 | $(3.88 \pm 0.07)10^{-6}$ | $0.685 \pm 0.021$ |
| +0.100 | $(4.24 \pm 0.05)10^{-6}$ | $0.569 \pm 0.012$ |

**Figure 23: Currents measured for NADH oxidation at six different potentials at a PANi-PAA modified electrode (deposition charge 236 mC cm$^{-2}$) plotted against the NADH concentration at a rotation speed of 9 Hz, in 0.1 M citrate-phosphate buffer pH 7, under argon. 100 mV vs SCE. The solid line represent the best fits of the experimental data to the expression for the case I-III boundary, the resulting kinetic parameters are given in the table.**

All subsequent experiments were performed at +0.05 V vs SCE. The effect of the film thickness is shown in Figure 24 for several film thicknesses. The film thickness is proportional to the charge passed to deposit the film. This was shown by measuring the thickness of PANi-PAA films deposited on glassy carbon electrodes using Scanning Electron Microscopy where a linear relationship was found:

$$Q_{growth}/\text{mC cm}^{-2} = 0.0211 \times L/\mu\text{m}.$$

From Figure 24 we can see that the catalytic currents increase with increasing film thickness and NADH concentration. This confirms that NADH oxidation occurs throughout the film. The data were fitted to the expression for the current across the I-II case boundary (thin film to thick films under unsaturated conditions).

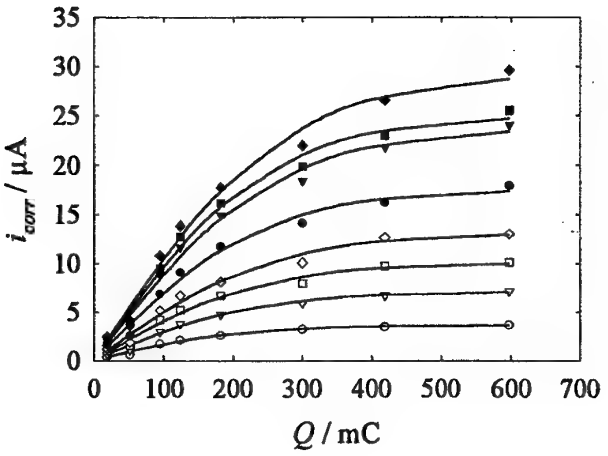


| $[NADH]_0$ / mM | $(k_{cat}[site]K_S^2D_S/K_M)^{1/2}$ / cm $s^{-1}$ | $(k_{cat}[site]\sigma^2/D_SK_M)^{1/2}$ / $C^{-1}$ |
|---|---|---|
| 0.05 | $(9.9 \pm 0.3) \times 10^{-4}$ | $4.9 \pm 0.4$ |
| 0.10 | $(9.8 \pm 0.3) \times 10^{-4}$ | $4.4 \pm 0.3$ |
| 0.15 | $(9.2 \pm 0.4) \times 10^{-4}$ | $4.2 \pm 0.4$ |
| 0.20 | $(8.9 \pm 0.4) \times 10^{-4}$ | $4.0 \pm 0.4$ |
| 0.30 | $(8.0 \pm 0.3) \times 10^{-4}$ | $4.2 \pm 0.4$ |
| 0.45 | $(7.2 \pm 0.3) \times 10^{-4}$ | $3.9 \pm 0.3$ |
| 0.50 | $(6.8 \pm 0.2) \times 10^{-4}$ | $4.1 \pm 0.3$ |
| 0.60 | $(6.7 \pm 0.3) \times 10^{-4}$ | $3.7 \pm 0.3$ |

**Figure 24: Currents for the oxidation of NADH at poly(aniline)-poly(acrylate) modified glassy carbon electrodes, geometric area 0.38 $cm^2$, coated with films of different thickness plotted as a function of the deposition charge. Results for eight different NADH concentrations are shown, recorded at +0.05 V at a rotation speed of 9 Hz, in 0.1 M citrate/phosphate buffer pH 7, under argon: ○ 0.05 mM; ▽0.1 mM; □ 0.15 mM; ◇ 0.2 mM; ● 0.3 mM; ▼ 0.45 mM; ■ 0.5 mM; ◆ 0.6 mM. The solid lines represent the best fits of the experimental data to the expression for the case III/IV boundary, the resulting kinetic parameters are given in the Table.**

We then find that the rotation speed has no significant effect on the catalytic currents (Figure 25), indicating that mass transport of NADH or $NAD^+$ in the bulk solution is not rate limiting, even at low NADH concentrations. The best fit parameters to the expression for the case IIII boundary are given in the table.

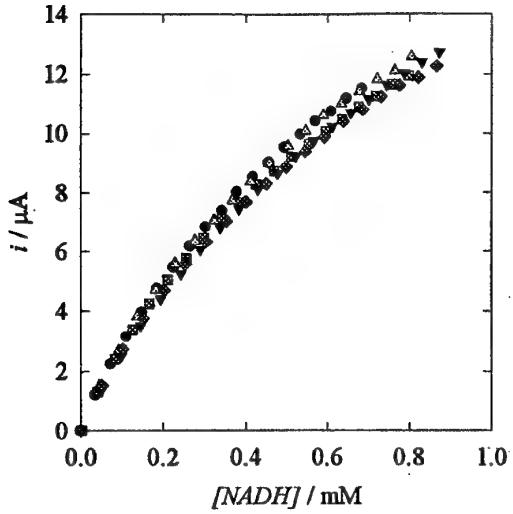


| $W$ / Hz | $nFAk_{cat}$[site]$\sigma$ / mol $s^{-1}$ $C^{-1}$ $cm^{-2}$ | $K_M/K_S$ / mM |
|---|---|---|
| 2 to 25 | 0.27 ± 0.004 | 0.76 ± 0.022 |

**Figure 25: Currents for the oxidation of NADH at poly(aniline)-poly(acrylate) modified glassy carbon electrodes (deposition charge 90 mC, geometric area = 0.38 $cm^2$) plotted as a function of NADH concentration, recorded at +0.05 V in 0.1 M citrate/phosphate buffer pH 7, under argon. Results for five different rotation speeds are shown: ● 2 Hz; ■ 4 Hz; ▲ 9 Hz; ▼ 16 Hz; ◆ 25 Hz.**

Finally $NAD^+$ inhibition was studied by adding $NAD^+$ to the bulk solution. It is clear from Figure 26 that $NAD^+$ inhibits the reaction and from the data we estimate the value $K_i/K_p$ as 8.2 mM.

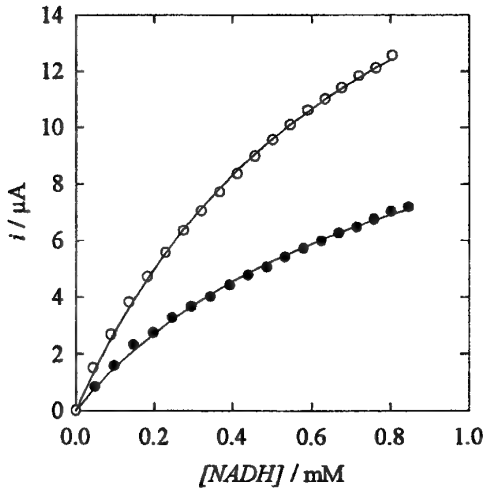


**Figure 26: Currents for the oxidation of NADH at poly(aniline)-poly(acrylate) modified glassy carbon electrodes (deposition charge 90 mC, geometric area = 0.38 $cm^2$) plotted as a function of NADH concentration, recorded at +0.05 V at a rotation speed of 9 Hz in 0.1 M citrate/phosphate buffer pH 7, under argon. Results recorded both in the absence (O) and in the presence (●) of 2.1 mM $NAD^+$ are shown.**

We compared the results we obtained for poly(aniline)-poly(acrylate) composite films with those for poly(aniline)-poly(vinylsulfonate) and poly(aniline)-poly(styrensulfonate) films. In all three cases, the mechanism is the same, NADH reacts at sites throughout the polymer film and there is reversible inhibition by the product, $NAD^+$. The oxidation process occurs around 50 to 100 mV vs SCE in the region where the poly(aniline) composite is conducting.

The catalytic currents observed at PANi-PAA coated electrodes are about one third of those at PANi-PVS films and about the same as those obtained at PANi-PSS modified electrodes, under the same conditions. In PANi-PVS, $K_M/K_s$ is smaller at +0.05 V than in PANi-PAA. This could be due to a larger $K_s$ value or a smaller value of $K_M$ and it is probably the results of differences in the morphology of the composites. The partition coefficient in both composites is probably not identical. If we suppose that the complex formation is about the same in both films, then we can conclude that $K_s$ is smaller in PANi-PAA, since $K_M/K_s$ is larger in this case than for PANi-PVS.

It is interesting to note that the PANi-PAA composite films are less easily inhibited by $NAD^+$ than the PANi-PVS films. This may be important for biofuel cell applications where a high concentration of $NAD^+$ may be present.

The different polymeric counter-ions can lead to differences in the electroactivity at pH 7. The fact that in PVS, a strong acid ($SO_3H$) is present and in PAA, a weak acid (COOH) cannot explain this difference; it is known that acetic acid can efficiently dope PANi [19, 20]. Nonetheless, poly(acrylic acid) is a buffer from pH 4 to 6.4, and the presence of anions and cations can influence the apparent $pK_A$ according to their size and concentration [21]. Thus protonated carboxylate groups may be present in PANi-PAA, and they cannot dope PANi at pH 7. Consequently doping with PAA is less efficient, and the concentration of catalytic sites will be smaller than in PANi-PVS composite films for a film of the same thickness. We believe, as a result of this, that the concentration of active catalytic sites within the film is smaller when using PANi-PAA as compared to PANi-PVS composite films. This is consistent with the differences in the resistance and the voltammetry of the two composite polymer films at pH 7.

Although poly(aniline)-poly(acrylate) films are not such good electrocatalysts as poly(aniline)-poly(vinylsulfonate) films for NADH oxidation, they do have the advantage

that the $NAD^+$ inhibition is less. In addition it should be possible to attach enzymes or modified cofactors to the polymer through linking to the carboxylate groups.

### *1.2.4. Hybrid films*

In order to improve the efficiency of the anode for use in a fuel cell it is desirable to operate at low overpotentials. It has been shown that 2,4,7-trinitrofluorenone (TNF), Figure 27, catalyses NADH oxidation at low overpotential (~-45 mV vs. Ag/AgCl) [22, 23]. We have therefore investigated the possibility of incorporating this mediator into the poly(aniline) composite films.

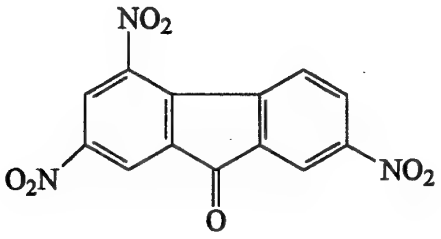


**Figure 27: Molecular structure of 2,4,7-trinitrofluorenone (TNF).**

The poly(aniline) films were first deposited on a glassy carbon electrode and then soaked in a solution of TNF in THF for 10 min. Then the TNF was activated by reducing one of the $NO_2$ group on the TNF to NHOH. The modified electrode was then used to study NADH oxidation. At 0.0V vs. SCE, a higher catalytic current (~2.5 times larger) was observed with the TNF/PANi-PAA modified electrode compared to the current observed under the same conditions with the PANi-PAA modified electrode (Figure 28).

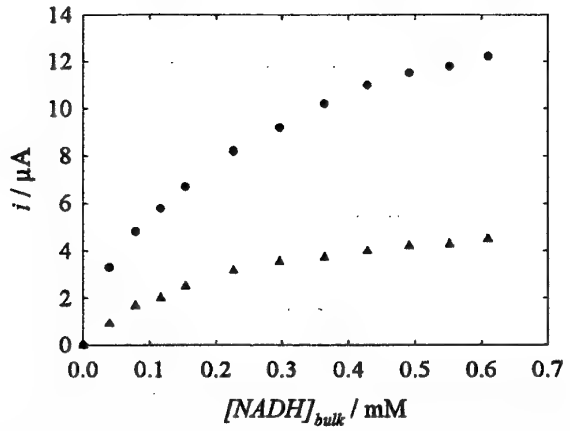


**Figure 28: Currents for the oxidation of NADH at poly(aniline)-poly(acrylate) modified glassy carbon electrodes (deposition charge 90 mC, geometric area = 0.38 $cm^2$) plotted as a function of NADH concentration, recorded at +0.00 V at a rotation speed of 9 Hz in 0.1 M citrate/phosphate buffer pH 7, under argon. Results recorded both in the absence of TNF in the PANi-PAA film (▲) or in the presence of TNF (●).**

Thus the incorporation of a trinitrofluorenone within in the poly(aniline) composite film is a viable way to lower the overpotential for NADH oxidation.

Nonetheless the weak adsorption of TNF on the PANi-PAA films make it difficult to get reproducible results. The attachment of TNF to the poly(aniline) composite films by a covalent bond would be a better solution.

## 2. *Kinetic isotope effect*

Since the poly(aniline)-poly(vinylsulfonate) films give highly reproducible modified electrodes, we measured the kinetic isotope effect for the oxidation of NADH at poly(aniline)-poly(vinylsulfonate) modified electrodes in order to probe in greater detail the mechanism of the catalytic reaction.

We replaced the two hydrogens in the 4-position of the nicotinamide ring of NADH by one or two deuterium atoms: [4,4-H,D]-NADH and [4,4-D,D]-NADH. Using our kinetic model we characterised the kinetic parameters for the oxidation of [4,4-H,D]-NADH and [4,4-D,D]-NADH on a poly(aniline)-poly(vinylsulfonate) composite film.

A kinetic isotope effect, $k_H/k_D$, had been used to define the mechanism of oxidation of NADH analogues, using different hydride acceptors. The oxidation of 1-benzyl-1,4-dihydromicotinamide by quinones has been studied by Miller. A kinetic isotope effect rising from 2.6 to 6.2 was found [24]. The authors concluded that the two quinones with a

$k_H/k_D$ of 2.6 adopted an electron-proton-electron mechanism, whereas for the others with a $k_H/k_D$ around 6, an direct hydride transfer could not be ruled out. A kinetic isotope effect of between 4.0 and 4.8 was found for the oxidation of BzNADH with N-methylacrinidinum ions [25]. Based on the temperature and substituent dependence of the isotope effect the authors concluded that tunneling made a significant contribution to the overall rate.

In order to use this model to characterise the mechanism of the oxidation of NADH at PANi-PVS composite films, we have to have conditions in which the rate reaction of the bound NADH is rate limiting at high concentration of NADH. Therefore we have to use the current expression for the I/III case boundary. To do this we used a thin film, varying the concentration of NADH from unsaturated to saturated conditions (up to 3-4 mM).

*Oxidation of β-Nicotinamide adenine dinucleotide, reduced form on PANi-PVS modified electrodes*

Poly(aniline)-poly(vinylsulfonate) composite films are easily deposited on glassy carbon electrodes and the modified electrodes show very reproducible electrochemical behaviour. We have used these composite films for the catalytic oxidation of NADH. Repeated amperometric experiments on the same film give the same catalytic currents for a NADH concentration up to 1 mM. Before performing kinetic isotope measurements on the poly(aniline) composite films, we first checked if it was possible to use the same film for three consecutive experiments and compared the kinetic data. Figure 29 shows the steady states currents observed for the oxidation of NADH (barium salt) at the same PANi-PVS film deposited on a glassy carbon electrode. The solid lines represent the currents calculated from the kinetic model, the kinetic data obtained are presented in table 1.

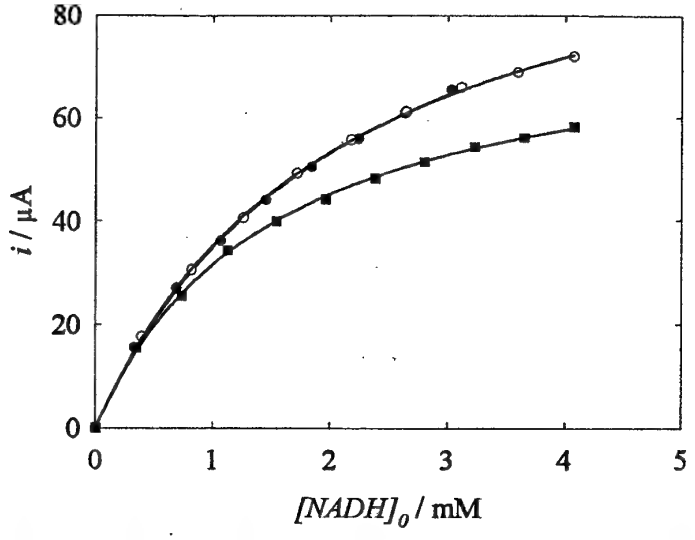


**Figure 29: Catalytic currents for NADH oxidation, recorded at 0.10V vs SCE at PANi-PVS modified electrode (electropolymerisation by cyclic voltammetry, deposition charge ~ 70 mC, geometric area = 0.38 cm$^2$, film thickness ~ 5 μm, ) rotated at 9 Hz in 0.1 M citrate/phosphate buffer pH 7.0 at 25 °C. First Run: (●); second run: (○), ; third run: (■), NADH.**

| | $k_{cat}$[site]σ / mol C$^{-1}$ s$^{-1}$ cm$^{-2}$ | $K_M/K_s$ / mM |
|---|---|---|
| Run 1 | (2.10 ± 0.05) x 10$^{-8}$ | 2.23 ± 0.10 |
| Run 2 | (2.05 ± 0.02) x 10$^{-8}$ | 2.12 ± 0.04 |
| Run 3 | (1.49 ± 0.02) x 10$^{-8}$ | 1.53 ± 0.0.4 |

**Table 1: Best fit parameters from the analysis of the currents for NADH oxidation at a poly(aniline)-poly(vinylsulfonate) modified glassy carbon electrode for three consecutive experiments, with the same film.**

The catalytic currents for the two first experiments are the same and the kinetic data, presented in table 1, show similar values. The third run shows that the catalytic currents are the same as the two previous experiments up to 1 mM, but above that concentration the catalytic currents observed dropped, probably due to some degradation of the composite film over time in buffer at pH 7.

We noticed from the data in table 1 and in Figure 29 that the same film can be used for NADH oxidation twice, without affecting the film (the redox charge measured after the first experiment showed no loss) or the kinetics of NADH oxidation. Therefore the site

concentration and the parameters characterising the film thickness are not affected by two consecutive experiments, consequently a change in the parameter, $k_{cat}$[sites]$\sigma$, is only due to the $k_{cat}$ parameter, and thus the rate of the oxidation of the bound NADH.

These experiments showed that the same PANi-PVS film could be used for repeated amperometric studies and gave similar kinetic data for the first two experiments. Thus the poly(aniline)-poly(vinylsulfonate) composite film can be used to measure the kinetic isotope effect for NADH oxidation under the same conditions.

*Kinetic isotope effect. Oxidation of β-Nicotinamide adenine dinucleotide-[4,4-(D,H)], reduced form*

Using a monodeuterated NADH, it may be possible to check if the poly(aniline) can distinguish between the two protons on the carbon in position 4 of the nicotinamide ring of NADH, that is whether the reaction is regioselective.

According to the literature, the monodeuterated compound prepared when using alcohol dehydrogenase is the *proR*-[4,4-(D,H)]-*β*-nicotinamide adenine dinucleotide, reduced form [26]. The amperometric responses obtained are shown on figure 30.

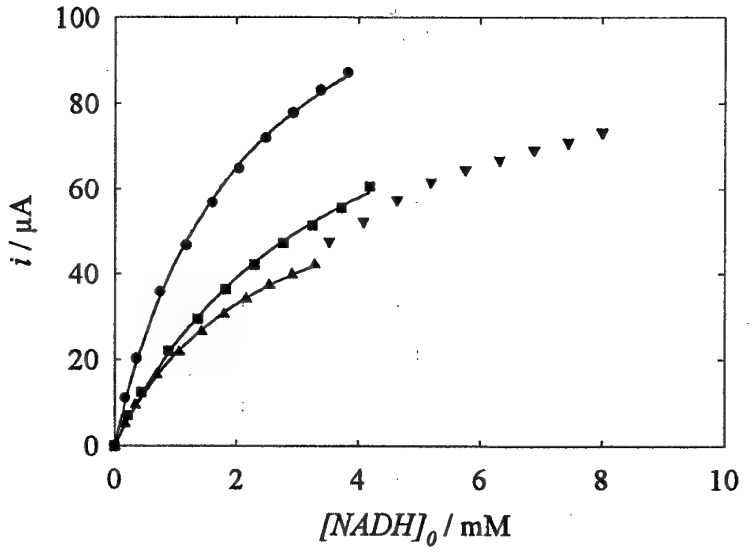


**Figure 30: Catalytic currents for NADH or [4,4-D,H]-NADH, recorded at 0.10V vs SCE at PANi-PVS modified electrode (electropolymerisation by cyclic voltammetry, deposition charge ~ 70 mC, geometric area = 0.38 cm$^2$, film thickness ~ 5 µm, ) rotated at 9 Hz in 0.1 M citrate/phosphate buffer pH 7.0 at 25 °C. First Run: (●) NADH; second run: (▲), [1,4-D,H]-NADH, (▼), NADH ; third run: (■), NADH.**

| | $k_{cat}$[site]σ / mol $C^{-1}$ $s^{-1}$ $cm^{-2}$ | $K_M/K_s$ / mM | $k_H/k_D$ |
|---|---|---|---|
| NADH | (2.60 ± 0.05) x $10^{-8}$ | 2.19 ± 0.09 | **1.87** |
| NADD | (1.39 ± 0.05) x $10^{-8}$ | 2.43 ± 0.10 | |

**Table 2: Best fit parameters from the analysis of the currents for NADH and [4,4-D,H]-NADH oxidation at a poly(aniline)-poly(vinylsulfonate) modified glassy carbon electrode for three consecutive experiments, with the same film.**

The currents for the second experiment are close to half of the currents observed for NADH. $K_M/K_S$ is not affected but $k_{cat}$[site]σ decreases (table 2). The measured kinetic isotope effect is 1.87, showing that the two sides of the nicotinamide ring of NADH cannot be distinguished by the poly(aniline) composite films. Presumably the binding of the NADH to the reaction sites is not strongly regioselective. This result is consistent with the isotope effect found for the [4,4-D,D]-NADH below.

*Kinetic isotope effect. Oxidation of β-Nicotinamide adenine dinucleotide-[4,4-(D,D)], reduced form*

To study the mechanism of NADH oxidation at poly(aniline)-poly(vinylsulfonate) composite films, dideuterated NADH was used instead of NADH. In figure 31, a large current drop is observed, when NADH is replaced by [4,4-D,D]-NADH in the second experiment. The corresponding kinetic parameters, $k_{cat}$[site]σ and $K_M/K_s$, are given in (table 3).

All the experiments were repeated in triplicate and a very good reproducibility was found. They were all performed in the same way: first a steady state experiment was performed with NADH (barium salt), second the experiment was repeated with [4,4-D,D]-NADH and then NADH are added to the cell at the end of this experiment, finally the experiment was repeated with NADH. In Figure 31 the catalytic currents are plotted against the NADH concentration. The NADH used was precipitated as the barium salt so as to be in exactly the same conditions as used for the [4,4-D,D]-NADH experiment. $Ca^{2+}$, $Ba^{2+}$, $Mg^{2+}$ are

known to enhance the catalytic currents observed for NADH oxidation when using different mediators [27-30]. Nonetheless in the present work, we found the same kinetic isotope effect when the disodium salt NADH was used, indicating that the effect of $Ba^{2+}$ was negligible.

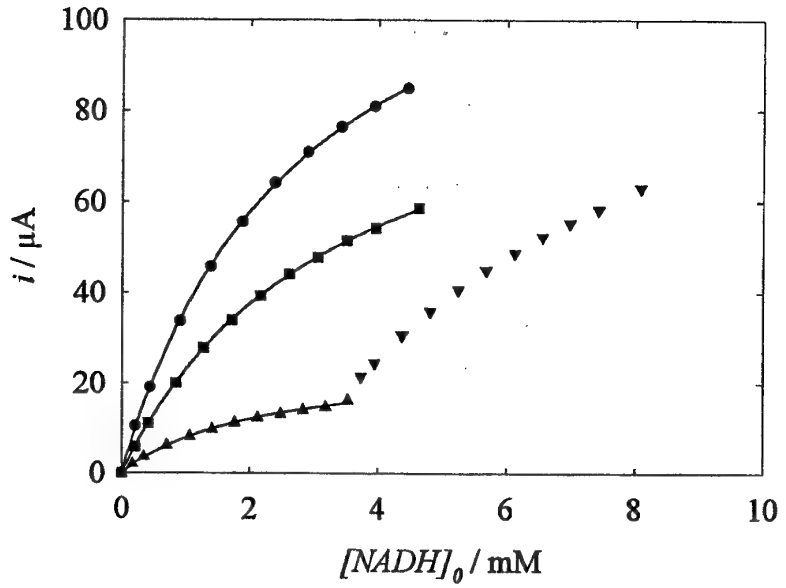


**Figure 31: Catalytic currents for NADH or [4,4-D,D]-NADH, recorded at 0.10 V vs SCE at PANi-PVS modified electrode (electropolymerisation by cyclic voltammetry, deposition charge ~ 70 mC, geometric area = 0.38 $cm^2$, film thickness ~ 5 μm) rotated at 9 Hz in 0.1 M citrate/phosphate buffer pH 7.0 at 25 °C. First Run: (●) NADH; second run: (▲), [1,4-D,D]-NADH, (▼), NADH ; third run: (■), NADH.**

| | $k_{cat}$[site]σ / mol $C^{-1}$ $s^{-1}$ $cm^{-2}$ | $K_M/K_s$ / mM | $k_H/k_D$ |
|---|---|---|---|
| NADH | (29.0 ± 0.30) x $10^{-9}$ | 2.77 ± 0.05 | **5.40** |
| NADD | (5.37 ± 0.20) x $10^{-9}$ | 2.24 ± 0.20 | |

**Table 3: Best fit parameters from the analysis of the currents for NADH and [4,4-D,H]-NADH oxidation at a poly(aniline)-poly(vinylsulfonate) modified glassy carbon electrode for three consecutive experiments, with the same film.**

From our results we found that $K_M/K_s$ does not change when [4,4-D,D]-NADH is used. Therefore the use of the deuterated compound does not affect the partition coefficient ($K_s$)

and the NADH binding to the catalytic site ($K_M$). The other parameter, $k_{cat}$[site]σ, is altered for the deuterated compound (table 3). The same film was used consecutively for a first experiment with NADH and a second one with [4,4-D,D]-NADH. As only the $k_{cat}$ is affected, we could measure the kinetic isotope effect, the parameters for the two experiments were found using our kinetic model (table 3). We found $k_H/k_D$ = 5.40, representing a primary kinetic isotope effect. This value is consistent with the values for hydride transfer in the literature [24, 25] and confirms that the cleavage of the C-H bond in the rate limiting step for the oxidation of the bound NADH.

No such kinetic isotope effect was observed on a bare glassy carbon electrode (Figure 32). For concentrations of NADH > 0.5 mM, the electrochemical oxidation occurs via the formation of $NADH^{+\bullet}$ radicals that can be adsorbed at the electrode surface, the product, $NAD^+$, can also be adsorbed at the electrode [31-35]. These phenomena are not reversible and lead to the fouling of the electrode. As shown on Figure 32, the catalytic currents for NADH or [4,4-D,D]-NADH are the same.

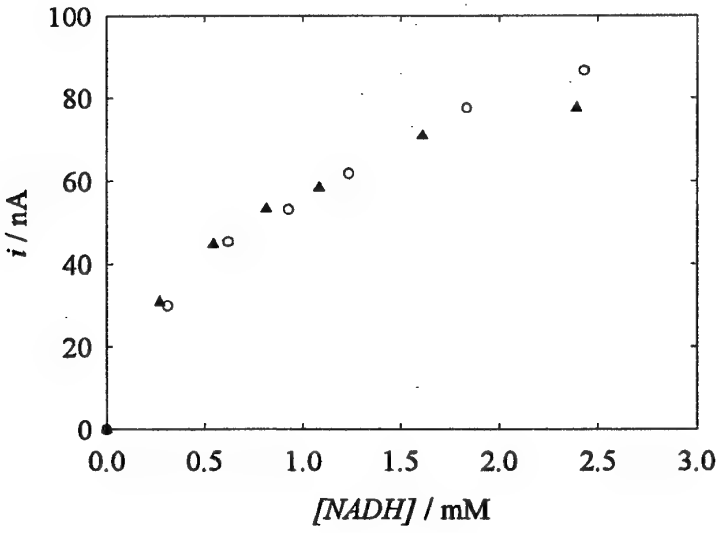


**Figure 32: Catalytic currents for NADH or [4,4-D,D]-NADH, recorded at 0.10 V vs SCE at bare glassy carbon electrode (geometric area = 0.38 $cm^2$ ) rotated at 9 Hz in 0.1 M citrate/phosphate buffer pH 7.0 at 25 °C. First Run: (○) NADH; second run: (▲), [1,4-D,D]-NADH.**

A kinetic isotope effect was measured for the oxidation of NADH at poly(aniline)-poly(vinylsulfonate) modified electrodes, using a kinetic model based on the diffusion of

NADH throughout the film and the kinetics of the reaction. The value obtained, 5.42, is similar to the values published for NADH analogues, and this high value confirms that a C-H bond is broken during the rate limiting step. Nonetheless, it is not possible at this stage to differentiate between a direct hydride transfer or an hydrogen atom transfer.

This is the first time, to the best of our knowledge, that a kinetic isotope effect has been used to study the mechanism of a reaction of any kind at a modified electrode.

## 3. *NADH analogue*

An NADH analogue, N-ethyl-1,4-dihydronicotinamide, was synthesised as part of the larger project by Bugg's group in Warwick. We then studied the oxidation of this analogue on poly(aniline)-poly(vinylsulfonate) modified electrode to confirm that they could be used with NADH analogues.

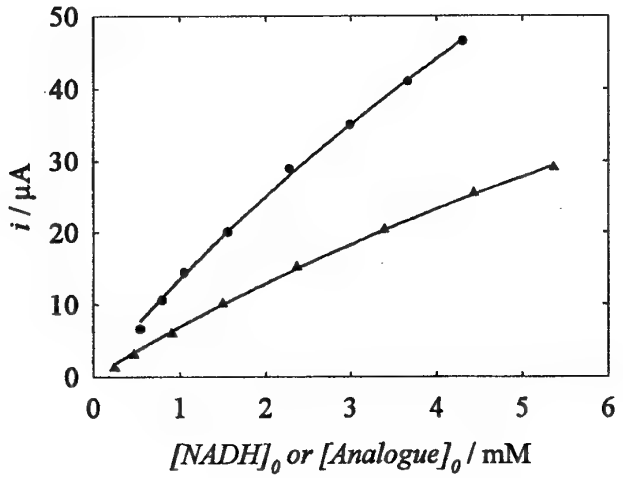


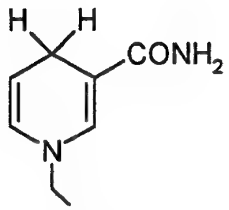


N-ethyl-1,4-dihydronicotinamide

**Figure 33: Catalytic currents for NADH or NADH analogue, recorded at 0.10 V vs SCE poly(aniline)-poly(vinylsulfonate) modified electrode (charge deposition = 125 mC, GCE, geometric area = 0.196 $cm^2$) rotated at 9 Hz in 0.1 M citrate/phosphate buffer pH 7.0 at 25 °C. (●) NADH analogue; (▲) NADH.**

The kinetic model was used to fit these data (I/II case boundary) and the results are collected in table 4.

| | $K_m/K_s$ / mM | $k_{cat}[site]D_sK_s$ / mol cm$^{-1}$ s$^{-2}$ |
|---|---|---|
| N-ethyl-1,4-dihydronicotinamide | 3.06 | $4.73 \times 10^{-13}$ |
| NADH | 3.84 | $1.49 \times 10^{-13}$ |

**Table 4: Best fit parameters from the analysis of the currents for NADH and N-ethyl-1,4-dihydronicotinamide oxidation at a poly(aniline)-poly(vinylsulfonate) modified glassy carbon electrode.**

The results show that the PANi composite films are good electrocatalysts for the oxidation of NADH analogues which appear to follow the same reaction mechanism as the parent compound. In this case the currents are larger for the analogue and the analysis of the data suggests that this is because the diffusion coefficient ($D_s$) for the reactant within the film is greater, presumably because the molecule is smaller. The data in table 4 suggest that the other parameters are probably the same for the two compounds.

## 4. *Enzyme immobilisation*

### 4.1 Cross-linking

Poly(acrylate) was chosen as dopant for poly(aniline) films for these experiments as the carboxylate groups of the poly(anions) could be used to attach molecules via an amide link.

PANi-PAA was deposited onto a glassy carbon electrode by electropolymerisation of aniline in the presence of PAA and HCl. The film formed was oxidised to the emeraldine (conducting) state. The electrode was washed with plenty of water and with PBS buffer solution pH 7. The modified electrode was immersed in a solution of EDAC (5 mg/ml in 100 mM PBS) for 1 hour at 4 °C. The electrode was then rinsed with plenty of water and phosphate buffer at pH 7.

NADH oxidation was studied at the surface of that modified electrode by chronoamperometry under the usual conditions (figure 34). Compared to the catalytic currents observed in the case of a PANi-PAA modified electrode without contact with

EDAC, the currents observed for NADH oxidation here are much lower. As the addition of $Ca^{2+}$ ions increased the catalytic currents observed for NADH at pH 7, the same experiment was carried out in 0.1 M Tris-HCl buffer pH 7 containing 10 mM of $CaCl_2$.

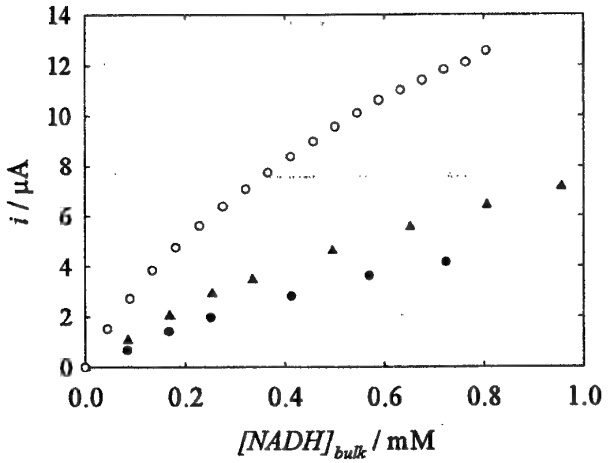


**Figure 34: Currents for the oxidation of NADH at poly(aniline)-poly(acrylate) modified glassy carbon electrodes (deposition charge = 104 mC, geometric area = 0.38 $cm^2$) plotted as a function of NADH concentration, recorded at +0.05 V at a rotation speed of 9 Hz in 0.1 M citrate/phosphate buffer pH 7 at 25 °C, under argon. Results recorded for a PANi-PAA film (O), for a PANi-PAA film exposed to EDAC (●) and for a PANi-PAA film exposed to EDAC (▲) in 0.1 M Tris-HCl pH 7.1, the presence of 10 mM $CaCl_2$ in the electrochemical cell.**

The catalytic currents are higher than in the phosphate buffer without calcium ions.

The plot of the catalytic current against the bulk concentration of NADH shows that the carbodiimide has an effect on PANi-PAA as the catalytic currents observed for PANi-PAA without contact with EDAC are higher.

The cross-linking agent can have an effect on the NH groups of PANi resulting in the cross-linking of PANi and PAA: the $COO^-$ groups of PAA being linked to the –NH- groups of PANi.

The presence of calcium gives higher catalytic currents. In subsequent experiments we tried to cross-link alcohol dehydrogenase to PANi-PAA films.

The expected reaction is described in Figure 35. The oxidation of enzymatically produced NADH is detected at the electrode, with PANi-PAA acting as the catalyst for the electrochemical oxidation of the NADH

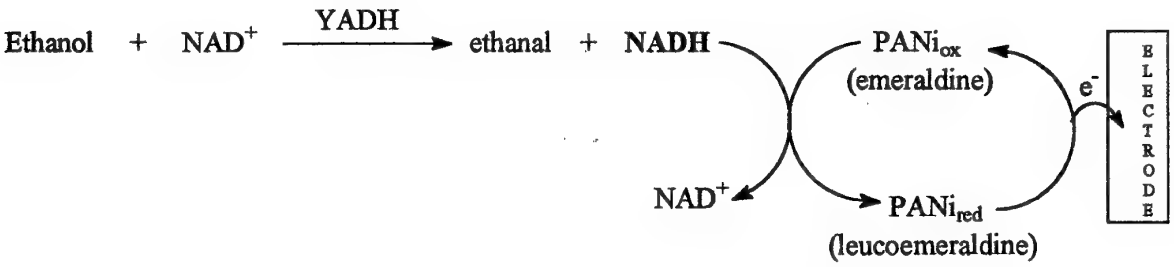


**Figure 35: Reaction at a YADH-PANi-PAA modified electrode.**

We used three different methods to cross-link YADH to PANi-PAA films (Figure 36):

1- The PANi-PAA was first activated by EDAC, then the enzyme was cross-linked. This method gave very low catalytic currents even at high ethanol concentrations.

2- The enzyme was activated by EDAC before being cross-linked to PANi-PAA. A catalytic current of ~1.7 μA at 3 M ethanol was obtained.

3- The EDAC was mixed with the enzyme and the PANi-PAA film was immersed immediately in the mixture. This method gave almost the same results as method 2 above.

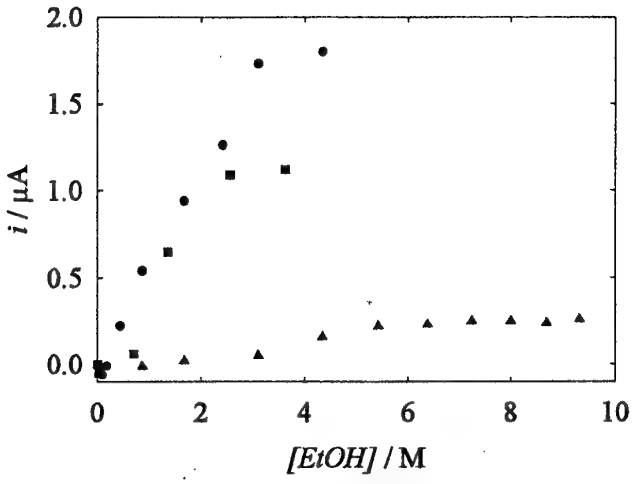


**Figure 36: Currents for the oxidation of NADH at poly(aniline)-poly(acrylate)-YADH modified glassy carbon electrodes (deposition charge 104 mC, geometric area = 0.38 $cm^2$) plotted as a function of ethanol concentration, recorded at +0.05 V at a rotation speed of 9 Hz in 0.1 M Tris-HCl + 10 mM $CaCl_2$ buffer pH 7.1 with 30 mM of $NAD^+$, at 35 °C, under argon. Results recorded when the PANi-PAA film is first activated by EDAC (▲) , when the enzyme was activated first (●) and when the film and the enzymes were activated at the same time (■).**

Since the catalytic currents are very small, even at very high concentrations of substrate, this enzyme immobilisation method was left aside.

Another way to immobilise the enzyme has been adopted: the introduction of a histidine tag on the C- or N-terminus of the enzyme to permit the immobilisation of the enzyme on a surface loaded with $Ni^{2+}$ ions. The histidine tag then forms a complex with the nickel (II) and immobilises the enzyme to the surface.

A poly(histidine) tag has been introduced at the C-terminal and N-terminal of a lactate dehydrogenase enzyme.

## 4.2 Mutant enzymes

Mutant enzymes, constructed and characterised by Dr Catherine Halliwell, Imperial College, have been immobilised on to these poly(aniline) composite films. LDH-CHis or LDH-NHis possess a C- or N-terminal hexahistidine tag. These enzymes have been immobilised on PANi-PAA films loaded with $Ni^{2+}$ ions. The $Ni^{2+}$ ions are then complexed by the histidine groups and thus the enzyme is immobilised onto the PANi-PAA-$Ni^{2+}$ film. Amperometric responses were recorded at LDH-PANi-PAA modified electrodes in the presence of $NAD^+$ and lactate at pH 7 (Figure 37).

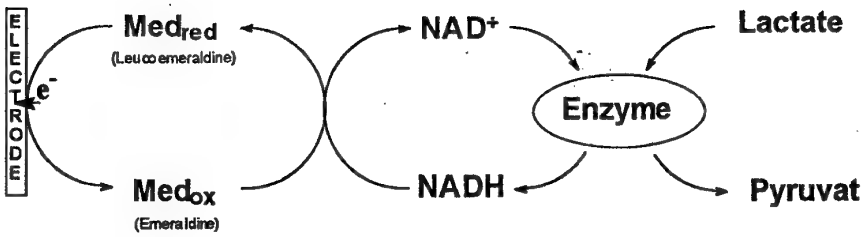


**Figure 37: Oxidation of enzymatically produced NADH at poly(aniline) modified electrodes.**

Some $Ni(SO_4)_2$ was dissolved in the electropolymerisation solution, and the PANi-PAA deposition was performed as usual. The presence of $Ni^{2+}$ in the PANi-PAA film was confirmed by atomic absorption.

The $Ni^{2+}$-PANi-PAA modified electrode was immersed in a solution of LDH-CHis for 4 hours. Then the electrode was thoroughly rinsed with water and buffer. It was then transferred to the electrochemical cell containing $NAD^+$ in 1.0 M L-lysine/acetic acid at pH 7 containing 10 mM $CaCl_2$. Aliquots of a 1 M solution of lactate were added in the cell and the catalytic current due to generation of NADH was detected.

The same experiment was performed with the enzyme in homogeneous solution rather that immobilised at the electrode surface; in this case the LDH-CHis was dissolved in 1.0 M L-lysine-acetic acid containing 30 mM $NAD^+$. For these experiments the PANi-PAA modified electrode was rotated at 4 Hz (Figure 38).

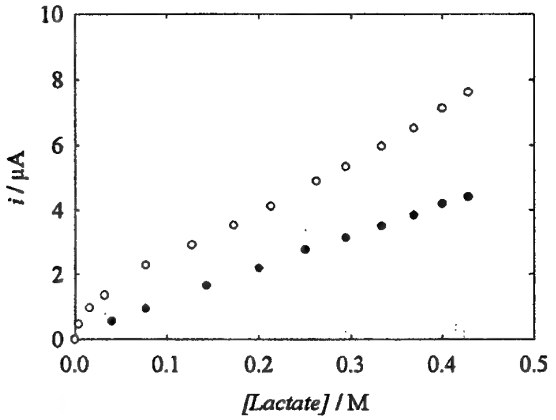


**Figure 38: NADH detection at a LDH-CHis-PANi-PAA modified electrode, LDH-CHis tagged to PANi-PAA or free in solution. $E_{applied}$ = 50 mV, $W$ = 9 Hz, in 1 M L-lysine-acetic acid + 10 mM of $CaCl_2$ pH 7.0 at 35 °C in presence of 17.7 mM of $NAD^+$. (●): LDH-CHis immobilized on PANi-PAA- $Ni^{2+}$; (○): 30 mM free LDH-CHis.**

Some catalytic currents were observed showing that the tag did work. Nonetheless the currents observed are very small. This may be due to loss of NADH from the electrode surface so that only a fraction of the NADH formed is detected at the electrode. It could also be due to there being only a small amount of LDH immobilised on the electrode in the absence of nickel (II).

Subsequent control experiments to investigate binding of the tagged protein to PANi-PAA, were performed in the absence of nickel. Unexpectedly, these revealed that in the absence of nickel (II) the chronoamperometric response was significantly greater for films of LDH-CHis than for the wild-type LDH (Figure 39).

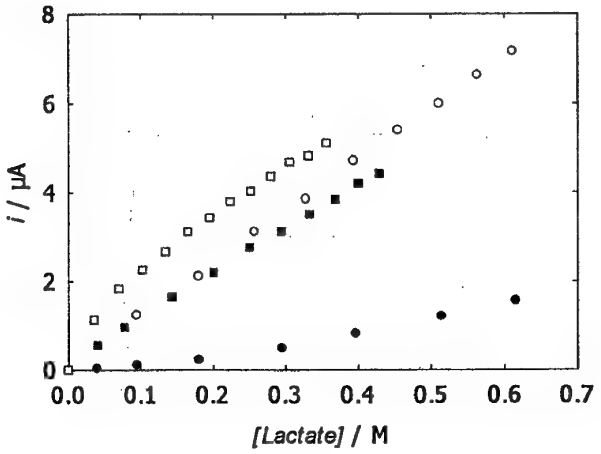


**Figure 39: Currents recorded at +0.05 V vs SCE at poly(aniline)-poly(acrylate) and $Ni^{2+}$ doped poly(aniline)-poly(acrylate) coated glassy carbon electrodes (deposition charge ~ 280 mC $cm^{-2}$, electrode area = 0.38 $cm^2$, thickness ~ 5.5 µm) rotated at 9 Hz in 1 M lysine, 10 mM $CaCl_2$, 30 mM $NAD^+$ at pH 7 and 35° C as a function of the lactate concentration. Data are corrected for background in each case. ● and ■ represent LDH-WT and LDH-CHis respectively, on $Ni^{2+}$ doped PANi-PAA film and ○ and □ represent LDH-WT and LDH-CHis respectively, on a standard PANi-PAA film.**

To show that the immobilisation of the tagged enzyme was stronger than the immobilisation of the wild-type enzyme, we repeated several times in a row the same experiment with the same film (Figure 40a). The same experiment was performed with the wild-type LDH, showing that after two experiments, a very low catalytic current is observed, suggesting that desorption of this enzyme occurs (Figure 40b). Note that this experiment cannot be done with the PANi-PAA film as it is stable for only one experiment, rather it was realised on a poly(aniline)-poly(vinylsulfonate) film, as this composite is much more stable towards repeated experiments.

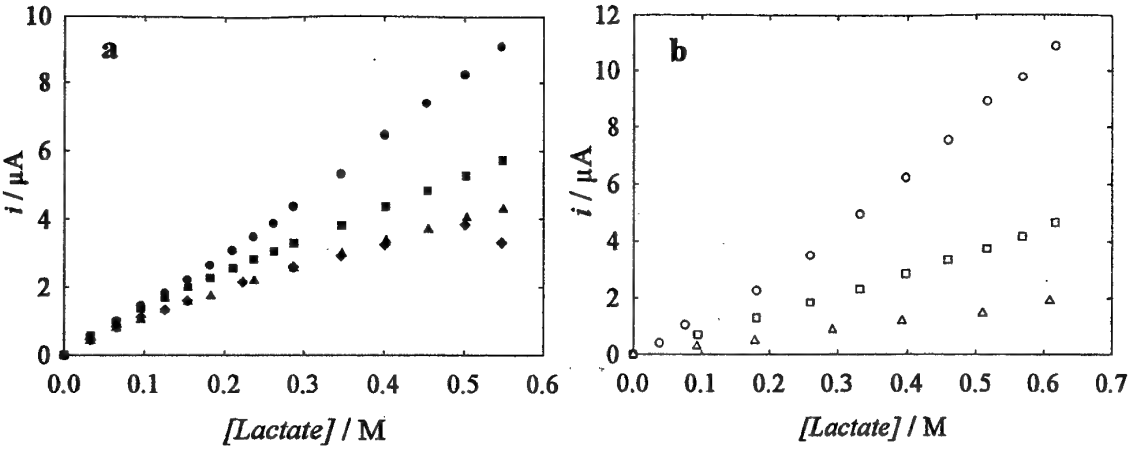


**Figure 40: Current recorded at +0.05 V vs SCE at poly(aniline)-poly(vinyl sulfonate) coated glassy carbon electrodes (electropolymerised by CV, deposition charge ~ 280 mC $cm^{-2}$, electrode area = 0.38 $cm^2$, thickness ~ 6.0 μm) at 9 Hz in 1 M lysine, 10 mM $CaCl_2$, 30 mM $NAD^+$ at pH 7 and 35 °C as a function of the lactate concentration. Data are corrected for background in each case. (a) ●, ■, ▲, ◆ represent run 1 to 4 respectively for LDH-CHis and (b) ○, □, △ represent runs 1 to 3 respectively for WT-LDH.**

The films of LDH-CHis immobilised on PANi-PVS produced higher NADH-dependent currents than the same film with the wild-type enzyme (Figure 41), despite the lower activity of the LDH-CHis mutant in solution relative to the wild type enzyme. Another mutant, with a poly(histidine) tag on the N-terminus (LDH-NHis), was prepared and this gave higher currents than either the LDH-CHis or WT-LDH.

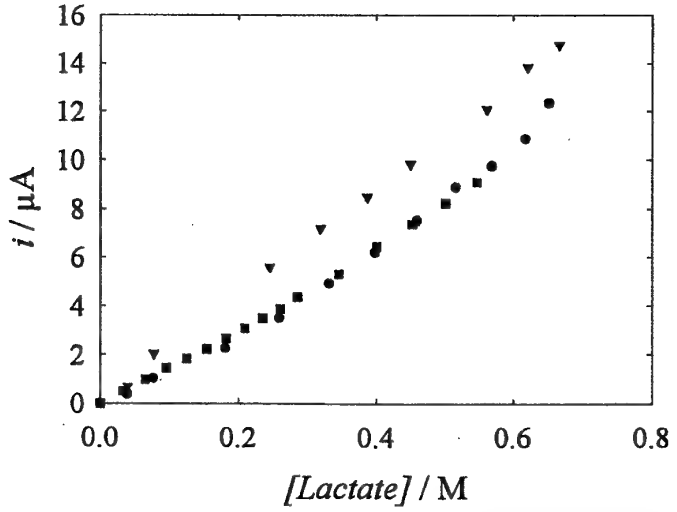


**Figure 41: Current recorded at +0.05 V vs SCE at poly(aniline)-poly(vinylsulfonate) coated glassy carbon electrodes (electropolymerised by CV, deposition charge ~ 280 mC $cm^{-2}$, electrode area = 0.38$cm^2$, thickness ~ 6.0μm) at 9 Hz in 1 M lysine, 10 mM $CaCl_2$, 30 mM $NAD^+$ at pH 7 and 35°C as a function of the lactate concentration. Data are corrected for background in each case. ●, ■ and ▼ represent LDH-WT, LDH-CHis and LDH-NHis respectively.**

We noticed that the buffer, 1M L-lysine, was not ideal for use around neutral pH and so we tried using Tris buffer. All the subsequent experiments were performed in 1.0 M Tris-HCl at pH 7.1. In Figure 42 we show the catalytic currents for NADH oxidation observed with the three forms of the enzyme, the wild-type LDH (WT-LDH) and LDH with a poly(histidine) tag on either the C-terminus (LDH-CHis) or the N-terminus (LDH-NHis). For both poly(histidine) tagged enzymes, the catalytic currents detected at any given lactate concentration are higher than those observed for the wild type enzyme. This is even though the LDH-CHis has only 64% of the substrate dependent activity of the WT-LDH, whereas the LDH-NHis is about as active as WT-LDH in homogeneous solution assays [36]. Of the two mutant enzymes the LDH-NHis shows a lower catalytic current than the LDH-CHis. This result is unexpected since the LDH-NHis was much more active than the LDH-CHis in spectrophotometric assays [36].

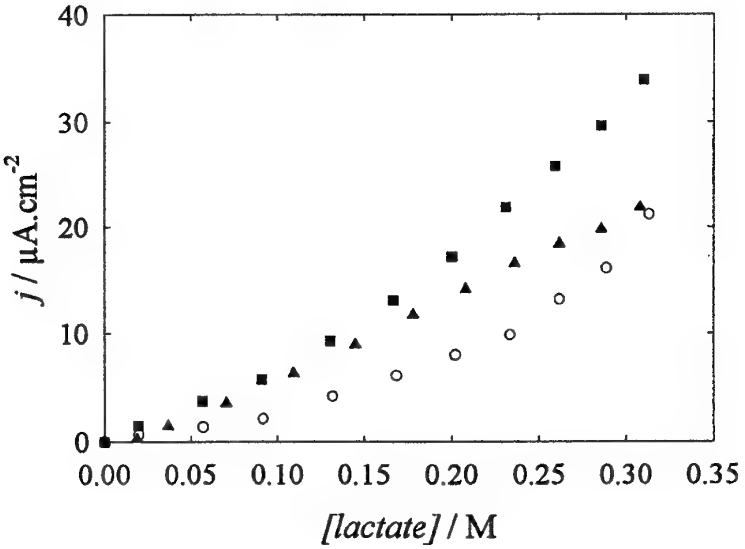


**Figure 42: Catalytic currents for enzymatically produced NADH, recorded at 0.05 V vs SCE at an enzyme/PANi-PAA modified electrode (electropolymerisation by cyclic voltammetry, deposition charge ~ 200 mC, geometric area = 0.38 $cm^2$, film thickness ~ 11 μm (measured by SEM), PANi-PAA film soaked in an enzyme solution (0.43 mg $ml^{-1}$) for 2 hours at 4°C) rotated at 9 Hz in 1.0 M Tris-HCl pH 7.1 at 35 °C, containing 30 mM $NAD^+$, under argon. O, ■ and ▲ represent WT-LDH, LDH-CHis and LDH-NHis respectively.**

We have checked the reproducibility of our results for the immobilisation of LDH using two different batches of enzyme. In order to compare the results for the catalytic currents in each case it is necessary to take into account the differences in the unit activity of the different batches of enzyme. This difference in enzyme activity is due to the variation in

the ratio of active to inactive LDH-CHis. As shown previously, the addition of a poly(histidine) tag to LDH produce a mixture of active and inactive enzyme [37] and the relative amounts of these two differ depending on the expression conditions. The activity of each batch of enzyme used was determined using a spectrophotometric assay [36] and the catalytic currents obtained in the different electrochemistry experiments were normalised. The $k_{cat}$ for LDH-CHis prepared in flasks is 91 $s^{-1}$ [36]. When a fermentor is used the proportion of inactive and active enzymes increases and the $k_{cat}$ was measured and found to be 50 $s^{-1}$. Figure 43 shows that different batches of enzyme give very similar results for the catalytic current for NADH generation when corrected (multiplied by 91/50) for the difference in the enzyme activity.

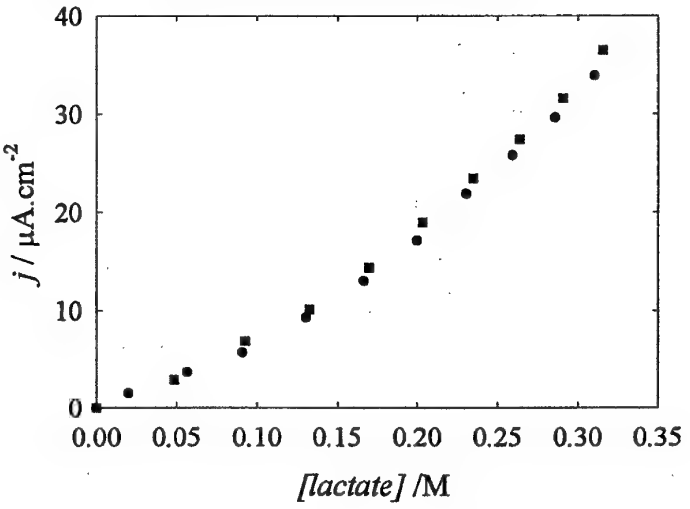


**Figure 43: Normalised catalytic currents for enzymatically produced NADH, recorded at 0.05V vs SCE at a LDH-CHis/PANi-PAA modified electrode (electropolymerisation by cyclic voltammetry, deposition charge ~ 200 mC, geometric area = 0.38 $cm^2$, film thickness ~ 11 μm (measured by SEM), PANi-PAA film soaked in a LDH-CHis solution (0.45 mg/ml) for 2 hours at 4 °C) rotated at 9 Hz in 1.0 M Tris-HCl pH 7.1 at 35°C, containing 30 mM $NAD^+$, under argon. Results are given for two different batches of LDH-CHis.**

The effect of the temperature on the current for oxidation of the enzymatically generated NADH was also investigated, Figure 44. At 25 °C, the catalytic currents observed were much lower than the those observed at 35 °C. We also increased the temperature to 45 °C. Although at low lactate concentrations the currents were the same at 45 °C as at 35 °C, above 0.1 M lactate the currents at 35 °C increase more rapidly with increasing lactate concentration. This is probably due to a denaturation of the enzyme immobilised on the film, since addition of NADH to the cell at the end of the experiment led to an increase of

the current, clearly showing that the PANi-PAA film was still active for NADH oxidation under these conditions. Although the native enzyme is from a thermophile so that no loss in activity should be observed up to 50°C it appears that it is less thermally stable when immobilised. All subsequent experiments were carried out at 35°C.

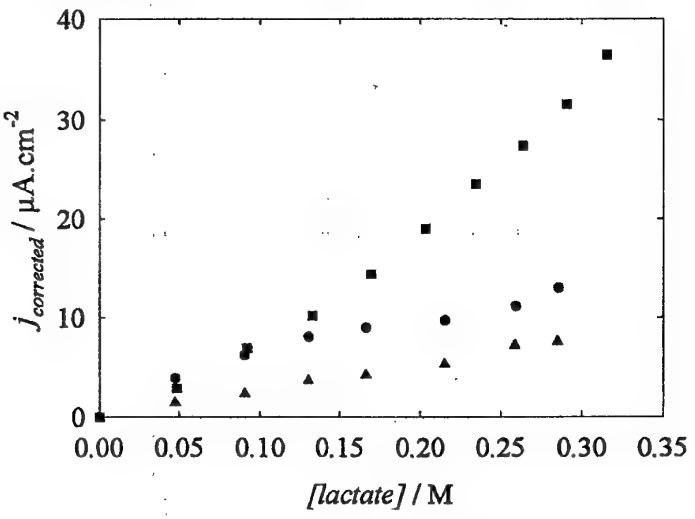


**Figure 44: Influence of the temperature on the catalytic currents for enzymatically produced NADH, at a LDH-CHis/PANi-PAA modified electrode (electropolymerisation by cyclic voltammetry, deposition charge ~ 200 mC, geometric area = 0.38 cm$^2$, film thickness ~ 11 µm (measured by SEM), PANi-PAA film soaked in a LDH-CHis solution (0.43 mg ml$^{-1}$) for 2 hours at 4°C) rotated at 9 Hz in 1.0 M Tris-HCl pH 7.1 containing 30 mM NAD$^+$, under argon, at 25(▲), 35 (■) and 45°C (●).**

We then investigated the effect of the concentration of the cofactor $NAD^+$ on the current. As shown in Figure 45 a decrease of $NAD^+$ concentration to 15 mM led to a decrease in the catalytic current. The high concentration of $NAD^+$ is necessary to shift the equilibrium in scheme 1 towards the production of NADH. Consequently in all the subsequent experiments we used 30 mM $NAD^+$.

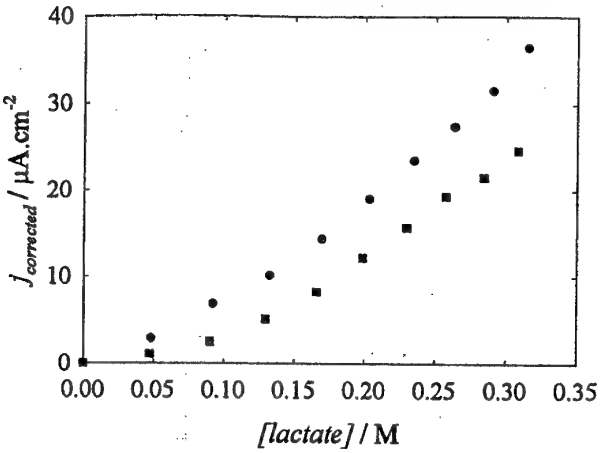


**Figure 45: Influence of the $NAD^+$ concentration on the catalytic currents for enzymatically produced NADH, at a LDH-CHis/PANi-PAA modified electrode (electropolymerisation by cyclic voltammetry, deposition charge ~ 200 mC, geometric area = 0.38 $cm^2$, film thickness ~ 11 μm (measured by SEM), PANi-PAA film soaked in a LDH-CHis solution (0.43 mg $ml^{-1}$) for 2 hours at 4 °C) rotated at 9 Hz in 1.0 M Tris-HCl pH 7.1 at 35 °C, containing 15 (■) or 30 mM (●) $NAD^+$, under argon.**

We then turned to the influence of the conditions used for the enzyme immobilisation. First we looked at the influence of the concentration of enzyme in the solution used to soak the film. As shown in Figure 46, when the concentration of the enzyme was reduced to 0.29 mg $ml^{-1}$, lower catalytic currents were observed, showing less production of NADH, presumably because less enzyme was immobilised on the PANi-PAA film. However increasing the concentration of the enzyme above 0.45 mg $ml^{-1}$ did not give any further increase in the catalytic currents (results not shown).

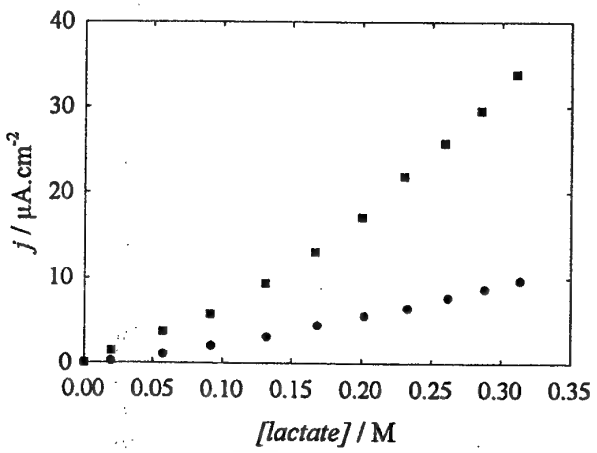


**Figure 46: Influence of the concentration of the LDH-CHis solution used to soak the poly(aniline) films) on the catalytic currents for enzymatically produced NADH, at a LDH-CHis/PANi-PAA modified electrode (electropolymerisation by cyclic voltammetry, deposition charge ~ 200 mC, geometric area = 0.38 $cm^2$, film thickness ~ 11 μm (measured by SEM), PANi-PAA film soaked in a 0.29 (●) or 0.44 (■) mg $ml^{-1}$ LDH-CHis solution for 2 hours at 4 °C) rotated at 9 Hz in 1.0 M Tris-HCl pH 7.1 at 35 °C, containing 30 mM $NAD^+$, under argon.**

We also varied the time taken to soak the electrode. As shown in Figure 47, 2 hours appears to be optimal. For shorter times, such as ½ hour or 1 hour, the catalytic currents observed were lower, presumably because the concentration of immobilised enzyme was less. Furthermore on soaking for 3½ hours the catalytic current was also lower, probably due to denaturation of the enzyme and deprotonation of the composite film over time.

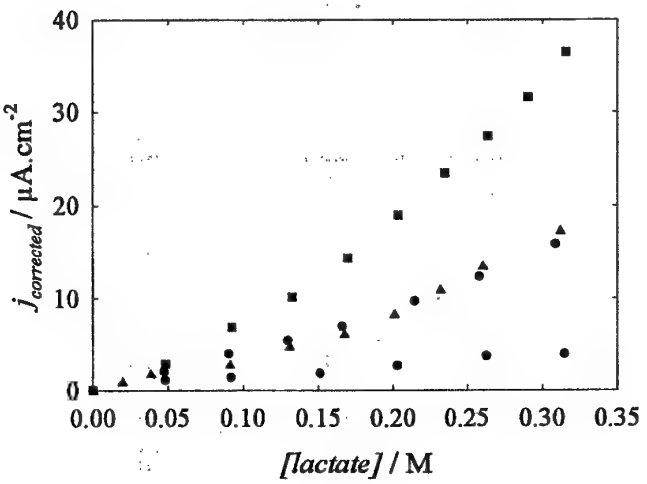


**Figure 47: Influence of the soaking time of the PANi-PAA composite film in a LDH-CHis solution on the catalytic currents for enzymatically produced NADH, recorded at 0.05 V vs SCE at a LDH-CHis/PANi-PAA modified electrode (electropolymerisation by cyclic voltammetry, deposition charge ~ 200 mC, geometric area = 0.38 cm$^2$, film thickness ~ 11 µm (measured by SEM), PANi-PAA film soaked in a LDH-CHis solution (0.43 mg ml$^{-1}$) for 30 min (▼), 1 (▲), 2 (■) or 3.5 (●) hours at 4°C) rotated at 9 Hz in 1.0 M Tris-HCl pH 7.1 at 35 °C, containing 30 mM NAD$^+$, under argon.**

To complete this part of our study, we looked at the influence of the PANi-PAA film thickness. The variation of the amperometric response as a function of the PANi-PAA film thickness is shown in Figure 48 for several different lactate concentrations.

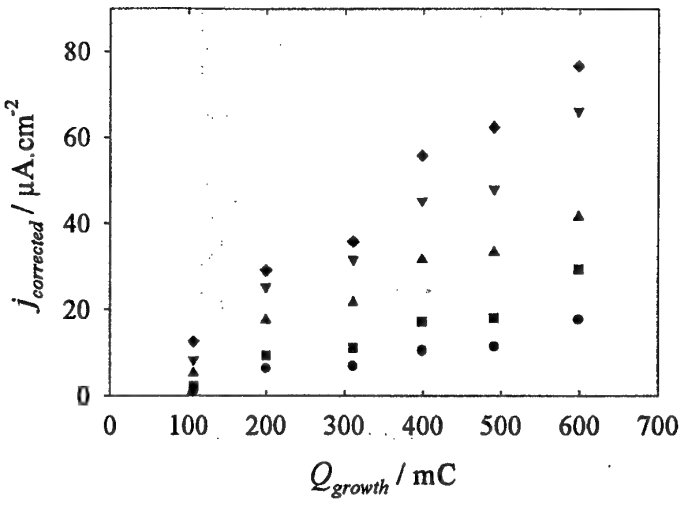


**Figure 48: Influence of thickness of the PANi-PAA composite film on the catalytic currents for enzymatically produced NADH, recorded at 0.05 V vs SCE at a LDH-CHis/PANi-PAA modified electrode (electropolymerisation by cyclic voltammetry, geometric area = 0.38 cm$^2$, PANi-PAA film soaked in a LDH-CHis solution (0.43 mg ml$^{-1}$) for 2 hours at 4 °C) rotated at 9 Hz in 1.0 M Tris-HCl pH 7.1 at 35 °C, containing 30 mM NAD$^+$, under argon. Results for 5 different concentrations of lactate are shown: ●, 0.09; ■, 0.13; ▲, 0.2; ▼, 0.26 and ◆, 0.3 M.**

In all cases the catalytic currents increase with the film thickness and with the lactate concentration, showing that the NADH oxidation occurs throughout the film as described previously [15]. This is consistent with the immobilisation of the enzyme and generation of NADH occurring throughout the film.

In order to find out if the immobilisation of the enzyme was dependent upon interactions between the enzyme and the poly(aniline) and/or with the poly(acrylate) counter-ion the same experiments were carried out using PANi-PVS composite films.

In previous works we have shown that poly(aniline)-poly(vinylsulfonate) films catalyse NADH oxidation at +0.1 V vs SCE and that the current densities for NADH oxidation at PANi-PVS films, for the same concentration of NADH, are approximately twice as large as those obtained at PANi-PAA films [6, 15]. As shown in Figure 49, when we immobilised LDH-CHis on the two films the catalytic currents observed for PANi-PVS were higher than those for PANi-PAA, but the difference between the two is smaller than expected based on their catalytic activities towards NADH oxidation. The catalytic currents observed with PANi-PAA are about two thirds of those obtained with PANi-PVS.

This could be explained by the fact that PANi-PAA is less inhibited by $NAD^+$ than PANi-PVS [15].

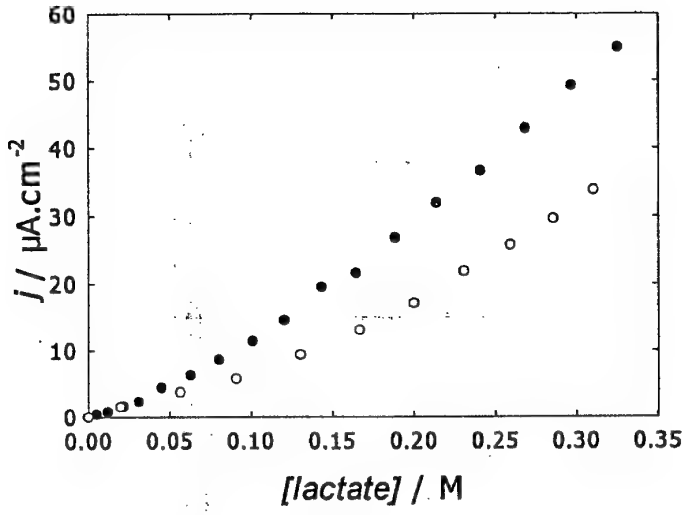


**Figure 49: Catalytic currents for enzymatically produced NADH, recorded at 0.05V vs SCE at a LDH-CHis/PANi-PAA (○) modified electrode or at 0.1 V vs SCE at a LDH-CHis/PANi-PVS (●) modified electrode (electropolymerisation by cyclic voltammetry, deposition charge ~ 200 mC, geometric area = 0.38 $cm^2$, film thickness ~ 11 µm for PANi-PAA and ~ 12 µm for PANi-PVS, PANi composite film soaked in an enzyme solution (0.43 mg $ml^{-1}$) for 2 hours at 4 °C) rotated at 9 Hz in 1.0 M Tris-HCl pH 7.1 at 35 °C, containing 30 mM $NAD^+$, under argon.**

The slight difference in the behaviour of PANi-PVS and PANi-PAA films can be attributed to their difference towards $NAD^+$ inhibition. We have studied the behaviour of these composite films towards NADH oxidation using a kinetic model in which we assume that NADH diffuses in the film, then forms a complex with catalytic sites within the film before being oxidised in $NAD^+$. This product, $NAD^+$ can compete with NADH to form a complex with the catalytic site and thus we also studied the effect of $NAD^+$ inhibition. We have shown that for PANi-PVS $K_i/K_p$ is 1.7mM and for PANi-PAA it is 8.2mM ($K_i$ is the inhibitor constant for reversible inhibition by $NAD^+$ and $K_p$ is the partition coefficient for $NAD^+$). A large value of this ratio indicates that the inhibition is only significant at high concentrations of $NAD^+$, and hence PANi-PAA is less inhibited by $NAD^+$ than PANi-PVS. In our experiments with lactate dehydrogenase we worked with a high concentration of $NAD^+$ (30 mM), so that the PANi-PVS film will show a greater inhibition than PANi-PAA The immobilisation of LDH mutants on poly(aniline) composite films seems independent of the counter-ion of the film (carboxylate or sulfonate).

As in the experiments with PANi-PAA described above, we immobilised both mutants, LDH-CHis and LDH-CHis, on PANi-PVS and compared the results to those obtained for the wild-type enzyme, Figure 50.

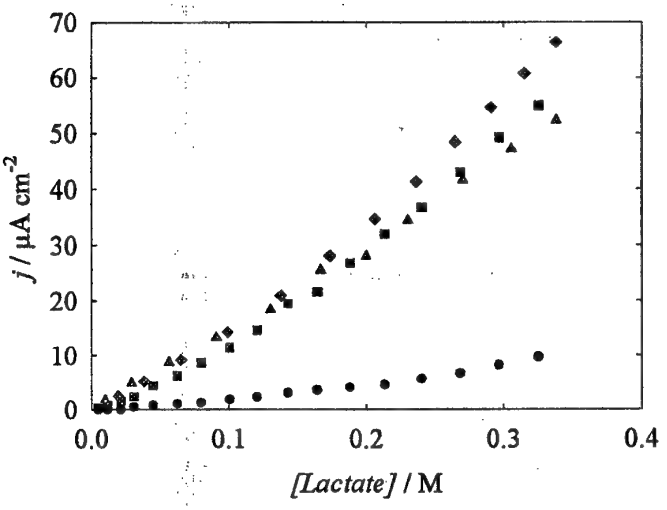


**Figure 50: Catalytic currents for enzymatically produced NADH, recorded at 0.10 V vs SCE at an enzyme/PANi-PVS modified electrode (electropolymerisation by cyclic voltammetry, deposition charge ~ 100 mC, geometric area = 0.196 $cm^2$, film thickness ~ 12 μm (measured by SEM), PANi-PVS film soaked in an enzyme solution (0.43 mg $ml^{-1}$) for 2 hours at 4 °C) rotated at 9 Hz in 1.0 M Tris-HCl pH 7.1 at 35 °C, containing 30 mM $NAD^+$, under argon. ●, ■, ▲ and ◆ represent WT-LDH, LDH-CHis, LDH-NHis and LDH-CCys respectively.**

In contrast to the results obtained on the PANi-PAA films this time the catalytic currents observed with LDH-NHis were greater than those for LDH-CHis. Again both mutants were more effective that the wild type enzyme. This difference between the two mutants could be due to differences in the enzyme activity or to greater adsorption for one of the mutants. As with LDH/PANi-PAA, the results obtained with PANi-PVS are reproducible for the different types of LDH. As poly(aniline) can undergo nucleophilic attack on its quinoneimine groups, a cysteine group was introduced on the C-terminal of LDH. In figure 49, we can see that this latter mutant gives the highest catalytic currents, although this mutant is much less active in solution than WT-LDH. This is probably due to a larger amount of enzyme being immobilised on the film. A method to quantify the amount of enzyme has been developed in which a radiolabelled leucine is introduced in the mutants during expression. The radiolabelled mutants are immobilised on the poly(aniline) composite films and then the radiolabel content is measured. This experiment were realised at Imperial College in Cass' group and is described in their report.

We also investigated the influence of the electrode rotation speed on the catalytic oxidation of NADH produced by LDH-CHis immobilised on PANi-PVS. For this experiment a single PANi-PVS film was used, the rotation speed was changed several times for the same concentration of lactate. As can be seen in Figure 51, the catalytic currents decreased when the rotation speed increased for the 3 different lactate concentrations used.

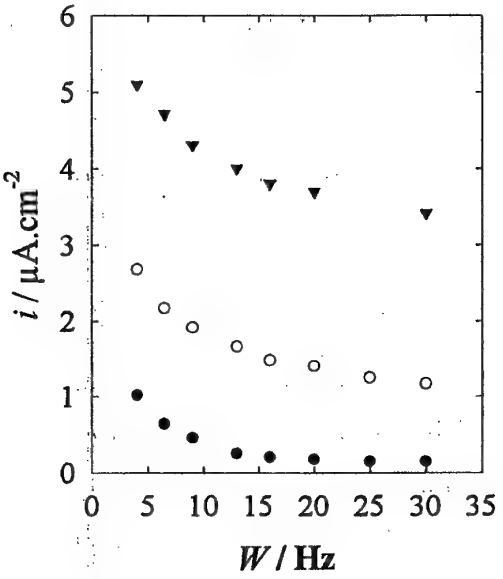


**Figure 51: Influence of rotation speed on the catalytic currents for enzymatically produced NADH, recorded at 0.10 V vs SCE at a LDH-CHis/PANi-PVS modified electrode (electropolymerisation by cyclic voltammetry, deposition charge ~ 100 mC, geometric area = 0.196 $cm^2$, PANi-PVS film soaked in a LDH-CHis solution (0.45 mg/ml) for 2 hours at 4 °C) rotated at 9 Hz in 1.0 M Tris-HCl pH 7.1 at 35 °C, containing 30 mM $NAD^+$, under argon. Results for 3 different concentrations of lactate are shown: O, 0.02; ●, 0.07 and ▼, 0.13 M.**

Between each measurement, the rotation speed was returned to 9 Hz and the current compared to that observed before changing the rotation speed. In every case the current was the same before and after changing the rotation speed, showing that the enzyme had not desorbed from the PANi-PVS film. The difference in the currents is probably due to a loss of NADH from the film when the rotation speed is higher. The NADH is directly produced at the film surface or within the film, an increase in the rotation speed results in more effective mass transport of NADH away from the electrode to the bulk solution and hence a lower current.

The immobilisation of the enzyme is probably the result of strong electrostatic binding. The presence of carboxylate group or sulfonate group in the PANi composite films makes

it possible to form ion pairs between these anions and amino groups on the enzyme. It has been shown that an organic sulfonate anion, 1-anilino-8-naphatlene sulfonate, is strongly bound to cationic groups of water-soluble proteins and aminoacids through ion pair formation [38]. The sulfonate present in PVS, or the carboxylate in PAA, could play the same role in the formation of ion pairs with LDH. The poly(aniline) composite films are sensitive to the pH and NADH is readily hydrolysed below pH 7, both factors make it very difficult to check the influence of pH on the LDH-CHis/PANi modified electrode to investigate the extent of ion pair formation.

When we compare the results obtained with the different mutants (LDH-CHis, LDH-NHis and LDH-CCys) and wild-type LDH we find that all the mutants give higher catalytic currents than wild-type LDH. This could be due to a stronger adsorption of the tagged enzyme compared to the wild-type LDH.

## 5. Conclusions

- Copolymers of aniline with anthranilic acid and with metanilic acid catalyse NADH oxidation, but the lack of reproducibility observed for the deposition of these materials would make it difficult to use them in a biofuel cell or in a biosensor. The catalytic activity of the best copolymers films was not significantly better that that for the poly(aniline)-poly(anion) composites.
- Poly(aniline)-Nafion® composite films are very stable at pH 7. When poly(aniline) is deposited within a precast Nafion® film the resulting composite is not permeable to anions. The co-immobilisation of poly(aniline) and Nafion® is more promising, but these composite films do not catalyse NADH oxidation although they do catalyse ascorbate oxidation. Nonetheless the catalytic currents observed for ascorbate oxidation were lower than those obtained with PANi-PVS or PANi-PAA composite films. A biofuel cell would require higher current densities and therefore PANi-Nafion® is not promising for this application. Nevertheless this composite might be useful in biosensors operating at neutral pH.
- NADH oxidation at poly(aniline)-poly(acrylate) films was studied in detail using a kinetic model originally developed for poly(aniline)-poly(vinylsulfonate) composite

films. This kinetic model remained valid for the new composite and kinetic parameters were obtained for the reaction of NADH at the poly(aniline)-poly(acrylate) electrode

- The poly(aniline)-poly(anion) films were shown to catalyse the oxidation of an NADH analogue (N-ethyl-1,4-dihydronicotinamide) by the same mechanism as NADH demonstrating that this approach could be used in a biofuel cell employing NADH analogues.
- Mono and dideuterated NADH samples were prepared and a significant kinetic isotope effect was found for their oxidation at poly(aniline)-poly(vinylsulfonate) composite films. The data were analysed in detail using our kinetic model. The kinetic isotope effect for oxidation of the dideuterated NADH in the bound complex was found to be 5.4, showing that cleavage of the C-H bond in the 4-position of the nicotinamide ring is involved in the rate limiting step. This strongly indicates that the oxidation of NADH to $NAD^+$ at PANi-PVS films, and by implication the oxidation of NADH analogues and the oxidation of NADH at other poly(aniline)-poly(anion) composite films, proceeds by a hydride transfer from the NADH to the PANi backbone.
- The immobilisation of two dehydrogenase enzymes on poly(aniline) composite films was studied. Cross-linking of yeast alcohol dehydrogenase to the carboxylate groups of a poly(aniline)-poly(acrylate) film led to very low catalytic currents in the presence of $NAD^+$ and alcohol due to a side-reaction between the poly(aniline) backbone and the cross-linking agent (EDAC). Therefore this method of enzyme immobilisation is not promising for our application.
- Engineered lactate dehydrogenase, bearing a poly(histidine) tag at the C- or N-terminus or a cysteine group, were prepared at Imperial College in Cass' group. These mutant enzymes appear to be strongly adsorbed on to poly(aniline)-poly(anion) composite films, probably through the formation of an ion pair. It is not necessary to add nickel(II) ions for the adsorption of the poly(histidine) tagged enzymes. When immobilised onto the poly(aniline) surface the engineered enzymes generate catalytic currents in the presence of the substrate (lactate) and $NAD^+$.
- Engineered dehydrogenase enzymes could be harnessed to operate as part of a biofuel cell using poly(aniline) based electrodes to catalyse the oxidation of the NADH. Remaining problems include the stability of the different components and optimisation of the operating potential and current density.

## 6. Refereed publications arising from this work

1. "Poly(aniline)-poly(acrylate) composite films as modified electrodes for the oxidation", P. N. Bartlett and E. Simon, *Physical Chemistry and Chemical Physics*, 2000, 2, 2599-2606.

2. "Modified electrodes for the oxidation of NADH", E. Simon and P.N. Bartlett, in "Biomolecular films: Design, Function, and Applications", J.F. Rusling (Ed.), Marcel Dekker Inc., New York, In press.

3. "The immobilisation of lactate dehydrogenase on poly(aniline)-poly(acrylate) and poly(aniline)-poly(vinylsulfonate) films for use in a lactate sensor", C. M. Halliwell, E. Simon, C.-S. Toh, P. N. Bartlett and A. E. G. Cass, *Anal. Chim. Acta*, **2001**, *in press*.

4. "Modified Electrodes for NADH Oxidation and Dehydrogenase Based Biosensors", P. N. Bartlett*, E. Simon and C. S. Toh, *Bioelectrochemistry*, 2002, accepted for publication.

5. "Immobilisation of enzymes on poly(aniline)-poly(anion) composite films. Preparation of bioanodes for biofuel cell applications", E. Simon, C. M. Halliwell, C.-S. Toh, A. E.G. Cass, P. N. Bartlett, *Bioelectrochemistry*, 2002, 55, 13-15.

6. "The Design of Dehydrogenase Enzymes for use in a Biofuel Cell: the Role of Genetically Introduced Peptide Tags in Enzyme Immobilisation on Electrodes", C. M. Halliwell, E. Simon, C.-S. Toh, A. E. G. Cass, and P. N. Bartlett, *Bioelectrochemistry*, 2002, 55, 21-23.

7. "Oxidation of NADH produced by a lactate dehydrogenase immobilised on poly(aniline)-poly(anion) composite films", E. Simon, C. M. Halliwell, C. S. Toh, A. E. G. Cass and P. N. Bartlett, *J. Electroanal. Chem.*, submitted.

8. "Measurement of a kinetic isotope effect at a poly(aniline) modified electrode". P. N. Bartlett and E. Simon, *J. Amer. Chem. Soc.*, manuscript in preparation.

## 7. Other output from this work

1. Lecture "Poly(aniline) composite films as mediators in NADH and ascorbate oxidation", P. N. Bartlett, E. Simon*, C.-S. Toh, E.N.K. Wallace, Electrochemistry'99, Portsmouth, UK, September 1999.

2. Poster presentation "Poly(aniline)-poly(anions) composite films: catalysts for electrochemical oxidation of NADH", P. N. Bartlett, E. Simon*, From Femto to Teraamps, Southampton, UK, 28-30 April 2000.

3. Poster presentation "Bioanode for Biofuel Cells. Immobilisation of Enzymes on Poly(aniline)-poly(anion) Composite Films", E. Simon*, C. M. Halliwell, C. S. Toh, P. N. Bartlett and A. E. G. Cass, Faraday Discussion: Bioelectrochemistry, Southampton, UK, July 2000.

4. Poster presentation "Kinetic Modelling of Dehydrogenase Enzyme Electrodes", C. S. Toh*, P. N. Bartlett, E. Simon, C. M. Halliwell and A. E. G. Cass, Faraday Discussion: Bioelectrochemistry, Southampton, July 2000.

5. Poster presentation "A rational-Design Approach to Enzyme Engineering and Immobilisation: The Design of Dehydrogenase Enzymes for use in a Biofuel Cell", C. M. Halliwell*, E. Simon, C. S. Toh, P. N. Bartlett and A. E. G. Cass, Faraday Discussion: Bioelectrochemistry, Southampton, July 2000.

6. Lecture "A Rational Design Approach to Enzyme Engineering and Immobilisation: The design of Dehydrogenase Enzymes for use in a Biofuel Cell", C. M. Halliwell*, A. E. G. Cass, E. Simon, C. S. Toh and P. N. Bartlett, Conference Proceedings of the International Symposium on Advances in Bioorganic Chemistry, Nov 20$^{th}$-24$^{th}$ 2000, Mumbai, India.

7. J. G. Patriarche Plenary Lecture "The molecular design of electrode surfaces", P. N. Bartlett*, ESEAC, Bonn, June, 2000.

8. Seminar "Applications of poly(aniline) in bioelectrochemistry", P. N. Bartlett*, Chulalongkorn University, Bankok Thailand, December 2000.

9. Plenary Lecture, "Modified electrodes for NADH oxidation and dehydrogenase based biosensors", P. N. Bartlett*, Bioelectrochemical Society, XVIth International Symposium on Bioelectrochemistry and Bioenergetics, Bratislava, June 2001.

10. Lecture "NADH oxidation with hybrid polyaniline/nitrofluorenone modified electrodes", A. Kuhn, N. Mano, P. Bartlett* and E. Simon, Joint ECS and ISE meeting, San Francisco, September 2001.

11. Lecture "Measurement of the kinetic isotope effect for the oxidation of NADH at a poly(aniline)-poly (vinylsulfonate) modified electrode", P. N. Bartlett* and E. Simon, to be given at 201$^{st}$ ECS meeting, Philadelphia, May 2002, accepted for oral presentation.

## 8. Appendix: materials and methods

All experiments were carried out in freshly prepared solutions using water purified by a Whatman RO 50 and a Whatman 'Still Plus' system. Aniline was distilled under vacuum and stored under argon at ~4 °C before use. Hydrochloric acid (Analar, BDH), potassium chloride (Analar, BDH), citric acid (Analar, BDH), disodium hydrogen orthophosphate dihydrate (Analar, BDH), hydrochloric acid (Analar, BDH), β-nicotinamide adenine dinucleotide, reduced form, di-sodium salt (NADH, ~98%, Sigma), β-nicotinamide adenine dinucleotide ($NAD^+$, ~98%, Sigma), L-lysine (98%, Sigma) and L-lactate, sodium salt (~98%, Sigma) were used without further purification. Tris(hydroxymethyl)-aminomethane (Tris) and hydrochloric acid were purchased from BDH (Analar grade).

Poly(acrylic acid), sodium salt solution in water, was purchased from Aldrich. Samples of three different molecular weights were used (1200, 8000, and 15000 Da). In each case the commercial solution was diluted with 4.0 M HCl to prepare a 15 wt.% solution of poly(acrylic acid) in 2.7 M in HCl. Solutions of pH 1 and 2 were prepared by mixing solutions of 0.1M HCl and 0.1 M KCl solutions. For pH from 3 to 7.5, buffer solutions were prepared by mixing solutions of 0.1 M citric acid and 0.2 M disodium hydrogen orthophosphate dihydrate [39]. All pH values were measured with a pH-meter (145 pH ion selective electrode probe, Corning) before use. UV-vis spectrophotometry (Hewlett-Packard 8452A UV-vis) was used to determine the concentration of all NADH solutions ($\varepsilon = 6220$ at 340 nm [40]).

All electrochemical measurements were made with an EG&G model 263A potentiostat in a conventional three electrode system. For rotating disc studies an Oxford Electrodes rotator and electrode was used. The working electrode was a glassy carbon rotating disc electrode (0.38 $cm^2$) used with a platinum foil counter electrode and a home-made saturated calomel electrode (SCE) reference electrode. All the potentials are reported with respect to SCE. Prior to use the working electrode was polished with an aqueous slurries of alumina (1.0 μm then 0.3 μm).

**Poly(aniline)-Nafion® composite films:**

*Electropolymerisation of aniline on precast Nafion® films*

A Nafion® film was cast from a commercial solution (Aldrich, 5 wt.% solution in lower aliphatic alcohols and water). A known volume of the solution was deposited with a micro-syringe on the electrode surface (0.38 $cm^2$). The solution was allowed to dry in air and room temperature overnight.

Polyaniline was electropolymerised from a 0.1 M solution of aniline in 1.0 M HCl by cyclic voltammetry, the potential was swept at 50 mV $s^{-1}$ from -0.2 to 0.9 V (5 cycles) and -0.2 to 0.78 V for the subsequent cycles until $Q_{deposition}$ = 110 mC. Different PANi film thickness were used.

Nafion precast film = 3µl equivalent to 0.2µm thick. PANi $Q_{deposition}$ = 110 mC

*Electropolymerisation of aniline in presence of Nafion®*

1 ml of the commercial solution of Nafion® was dissolved in 1 ml of methanol and 0.5 ml of aniline is dissolved in 2 ml of 1.0 M HCl. The aniline solution was slowly added to the Nafion® solution, and 7.5 ml of 1.0 M HCl were added. A lot of bubbles were formed during the process, the electropolymerisation was performed after they have disappeared.

The composite film was deposited by cyclic voltammetry, 1st cycle: -0.2 to 0.9 V then -0.2 to 0.78 V at 50 mV $s^{-1}$ until the required charge was obtained. If the potential is simply swept from -0.2 to 0.8V the polymer growth is very slow.

**Poly(aniline)-poly(acrylate) composite films**

Electropolymerisation of aniline was performed at room temperature from a solution containing 0.5 M of aniline, 15 wt.% PAA and 2.7 M HCl (5 ml of the commercial solution of PAA mixed with 10 ml of 4.0 M HCl). The electrode potential was swept from –0.2 to 0.9 V for the first cycle and then from –0.2 to +0.78 V for all subsequent cycles, at 50 mV $s^{-1}$. The deposition charge was recorded during the electropolymerisation process, when the desired charge was reached, the experiment was stopped, and the electrode was rinsed with water and 1.0 M HCl solution.

Poly(aniline)-poly(vinylsulfonate) composite film were electropolymerised from a 0.5 M solution of aniline in 22.4% PVS and 1.0 M $H_2SO_4$ (4.7 ml of the commercial solution of

PVS and 0.3 ml of concentrated $H_2SO_4$). PANi-PVS films were deposited on a glassy carbon electrode by cyclic voltammetry under the same conditions used for PANi-PAA.

**Catalysis of NADH oxidation at poly(aniline)-poly(anion) composite films**

The amperometric response to NADH was studied in a water jacketed thermostated cell (25.0 ± 0.1 °C), in deoxygenated solution under argon or nitrogen at a fixed potential. Prior to each experiment the poly(aniline) composite film coated electrode was preconditioned at +0.5 V in 1.0 M HCl for five min. The electrode was then rinsed with water and pH 7 buffer solution, and then immersed in the electrochemical cell containing deoxygenated pH 7 buffer solution. The electrode was rotated and the potential held at the chosen potential (usually +0.05V and +0.1 V vs SCE for PANi-PAA and PANi-PVS respectively) while aliquots of a stock solution of NADH (0.01 M in buffer solution) were added to the cell. The resulting steady state catalytic currents were recorded.

**UV-Visible characterisation of PANi-PAA and resistance measurements**

For UV-visible characterisation PANi-PAA films were deposited on an ITO-glass electrode, using the same procedure as described above. The films were dried at 40 °C and the UV-vis spectra recorded.

For the *in situ* resistance measurements, a PANi-PAA film was deposited across the gap between 2 screen printed carbon microband electrodes, as described in the literature [6].

**Kinetic isotope effect measurement**

*β-Nicotinamide adenine dinucleotide-[4,4-(D,H)], reduced form*

The deuteration of NADH was performed as described by Brown *et al.* [41]. 0.6 g of $NAD^+$ were dissolved in 14 ml of 0.5 M unadjusted Tris. 0.8 ml of $C_2D_5OD$ and 8 mg of yeast alcohol dehydrogenase dissolved in 1 ml of Tris were added under stirring. The UV-visible absorption at 340 nm was recorded, when the maximum absorption was obtained the reaction mixture was boiled for 5 min. The solution was then filtered and 1.5 ml of a 25 wt% barium acetate was added. Cold absolute ethanol (40 ml) was finally added, and a

white precipitate formed. The solution was placed on ice for 2 hours, then the solid was collected and washed with ethanol, ethanol-ether (1:1) and finally ether. The yellowish solid obtained was then dried under vacuum. Yield = 72%.

Before using [4,4-D,H]-NADH in electrochemistry experiments, it was redissolved in 0.1 M unadjusted Tris, and some cold ethanol added. The solution was placed on ice for 2 hours, then the precipitate was collected and washed with ethanol and ether and then dried for 12 hours under vacuum.

$^1$H NMR: 8.1 (s, 1H); 8.3 (s, 1H); 6.8 (s, 1H); 5.8 (d, 1H); 5.9 (d, 1H); 4.8 (m, 9H); 4.2 (m, 10H); 3.5 (q, 1H) and 2.6 ppm (d, 1H on $C_4$)).

The change in the peaks at 2.6 ppm showed that the NADH had been deuterated on the $C_4$ position. Before the second precipitation, the compound is deuterated to more than 95%.

Mass spectrometry: $m/z$ = 665.1

Elemental analysis:

| | |
|---|---|
| Calculated | C: 31.5%; H: 3.3%; N: 12.2%; P: 7.27% |
| Found | C: 29.06%; H: 3.95%; N: 11.33%; P: 7.62%, |

*β-Nicotinamide adenine dinucleotide-[4,4-(D,D)], reduced form*

The stereoselectivity of dehydrogenase enzymes is used to prepared stepwise [4,4-D,D]-NADH in a stepwise synthesis.

0.67g of [4,4-D,H]-NADH and 0.11 g of $Na_2SO_4$ were dissolved in 10 ml of phosphate buffer at pH 7.6. The solution was filtered and the white precipitate discarded. 0.2 g of ammonium chloride and 0.3g of α-ketoglutaric acid were mixed with the NADH solution under stirring. Finally 3 mg of L-glutamic acid in a solution of 1 ml of phosphate buffer solution was added. The pH was maintained by adding 0.1 M HCl. The absorption spectrum was recorded and the reaction was stopped when the peak at 340 nm disappeared. Then the solution was acidified to pH 2 by adding 2.0 M HCl. Cold acetone was then added, a white precipitate formed, and the solution was kept at 4-5 °C for 3 hours. The precipitate is very hygroscopic and difficult to isolate. Therefore it was quickly dried by a flux of argon, then redissolved in 5 ml of 0.5 M unadjusted Tris. We then proceeded as in the synthesis of [4,4-D,H]-NADH described above. 0.6 ml of $C_2D_5OD$ and 6 mg of ADH were added and the UV-vis spectra were recorded until reaction completion. The reaction mixture was boiled for 5 min, filtered and 1 ml of a 25 wt% barium acetate solution was added. The addition of cold absolute ethanol led to the precipitation of a white solid. The

solution was placed on ice for 2 hours. The precipitate was collected and washed with ethanol, ethanol:ether (1:1) and ether before drying under vacuum.

The solid was redissolved in 0.1 M unadjusted Tris, and some cold absolute ethanol was added to precipitate the NADD as a barium salt. The solution was placed on ice for 2 hours and the precipitate was collected, washed with ethanol and ether and then dried under vacuum for 12 hours. The [4,4-D,D]-NADH obtained was used without further purification. The total yield was 45%.

$^1$H NMR: 8.1 (s, 1H); 8.3 (s, 1H); 6.8 (s, 1H); 5.8 (d, 1H); 5.9 (d, 1H); 4.8 (m, 9H); 4.2 (m, 10H); and 3.5 ppm (q, 1H).

The disappearance of the peaks at 2.5 ppm showed that the NADH had been deuterated on the $C_4$ position. The deuteration is complete (more than 99%).

Mass spectrometry: m/z=665.1, $M^{\ominus}$+D = 666.2

Elemental analysis:

Calculated C: 31.5%; H: 3.1%; N: 12.2%; P: 7.27%

Found C: 26.42%; H: 3.75%; N: 9.11%; P: 7.27%,

*Precipitation of β-Nicotinamide adenine dinucleotide-[4,4-(D,D)], reduced form as the barium salt*

As the deuterated compounds are used as the barium salt, commercial NADH was also precipitated as the barium salt for direct comparison. 0.6 g of NADH was dissolved in 8 ml of 0.1 M unadjusted Tris and 1.5 ml of a 25 wt% barium acetate solution was added. The addition of cold absolute ethanol led to the precipitation of a white solid. The solution was placed on ice for 2 hours. The precipitate was collected and washed with ethanol, ethanol:ether (1:1) and ether before drying under vacuum.

The poly(aniline)-poly(vinylsulfonate) composite films were deposited by cyclic voltammetry on a glassy carbon electrode as described above.

The poly(aniline)-poly(vinylsulfonate) modified electrodes were placed in a thermostated cell held at 25 °C, containing 3 ml of 0.1 M citrate-phosphate buffer at pH 7.0. The electrode was rotated at 9 Hz unless and the potential held at 0.10 V vs SCE. Aliquots of a concentrated solution of NADH in citrate phosphate buffer (150 µl of a 60 mM solution were prepared in 0.1 M citrate-phosphate buffer and the solution was filtered on cotton wool) were added to the electrochemical cell and the steady state catalytic currents were recorded. After the first experiment, the poly(aniline)-poly(vinylsulfonate) modified

electrode is thoroughly rinsed with 10 ml of 0.1 M citrate-phosphate buffer pH 7.0, and placed immediately in to a cell containing 3 ml of the buffer solution at 25 °C under argon and the next experiment was performed immediately.

**Enzyme Cross-linking**

Chemicals: Aniline (from BDH) was distilled under vacuum, and kept in the fridge under argon. 1-Ethyl-3-(3-dimethylaminopropyl)carbodiimide (EDAC) was purchased from Aldrich. Poly(acrylic acid, sodium salt) (Mw = 8000 Da) 45 wt% solution was diluted in 4 M HCl to prepare a 15 wt% solution. The buffer solutions used were of analytical grade.

Electropolymerisation process: deposition of PANi-PAA composite films onto glassy carbon electrode.

0.5 M of aniline was dissolved in 15 wt% PAA solution. The aniline electropolymerisation was obtained by cyclic voltammetry: first cycle –0.2 to +0.9 V, subsequent cycles: -0.2 to 0.78 V (not 0.9 V to avoid degradation of PANi). $\nu$ = 50 mV $s^{-1}$. The process was stopped when the charge obtained reaches the desired value (usually 90 mC for a GCE, area = 0.38 $cm^2$).

Emeraldine state: the PANi-PAA film is conducting in its emeraldine state (semi-oxidised). To ensure that the whole film was in this redox state, the potential was held at +0.5 V in 1.0 M HCl for 5 min.

Cross-linking: the cross-linking agent used was 1-Ethyl-3-(3-dimethylamino-propyl)carbodiimide (EDAC), in solution in PBS buffer pH 7.4. Different methods were are used: activation of the PANi-PAA first followed by addition of the enzyme; putting the PANi-PAA, EDAC and enzyme in same solution all together at the same time; or activation of the enzyme first.

**LDH mutants**

Poly(aniline)-poly(acrylate) or poly(aniline)-poly(vinyl sulfonate) films of known thickness were deposited on the electrodes according to the method described above. All films were deposited to approximately the same thickness, which was calculated from the charge measured for the films both during deposition and acid cycling. A film of 5 μm thickness was usually deposited, corresponding to a charge of 90 mC at the end of the

deposition. The charge was measured both during electropolymerisation and also during cycling in 1 M hydrochloric acid.

For films that incorporated $Ni^{2+}$, 0.1 M $NiSO_4$ was added to the electropolymerisation solution. All films were equilibrated in the emeraldine state by holding the electrode at a fixed potential (0.5 V for 300 s) in 1 M HCl immediately prior to enzyme immobilisation. The electrode was then rinsed with water and suspended in a solution of the tagged enzyme (1mg/ml of the enzyme in 0.1 M sodium phosphate, pH 7.1) for 2 hours at 4°C. The electrode was then extensively rinsed with sodium phosphate buffer and air-dried.

The electrochemical assay solution (30 mM $NAD^+$, in 1 M lysine, 10 mM $CaCl_2$, pH 7.0) was thoroughly degassed and equilibrated at 35 °C for 20 min. The enzyme electrode was then immersed in this solution and equilibrated at 0.05 V for 20 min or until the anodic current stabilised, at a rotation speed of 9 Hz. Aliquots of sodium lactate were then added (to a final concentration of 0.5 M) and the NADH dependent current measured.

## 9. References


1. P. Bartlett and K. Pratt, J. Electroanal. Chem. 397:53 (1995).
2. E. Simon and P. N. Bartlett, in Biomolecular films: design, function and applications (J. F. Rusling, ed.), Marcel Dekker Inc., New York, in press.
3. R. M. Penner and C. R. Martin, J. Electrochem. Soc. 133:310 (1986).
4. T. Hirai, S. Kuwabata, and H. Yoneyama, J. Electrochem. Soc. 135:1132 (1988).
5. G. Nagasubramanian, S. D. Stefano, and J. Moacanin, J. Phys. Chem. 1986:4447 (1986).
6. P. N. Bartlett, P. R. Birkin, and E. N. K. Wallace, J. Chem. Soc., Faraday Trans. 93:1951 (1997).
7. P. N. Bartlett and E. N. K. Wallace, J. Electroanal. Chem. 486:23 (2000).
8. D. Orata and D. A. Buttry, J. Electroanal. Chem. 257:71 (1988).
9. Y.-J. Cho and H.-J. Huang, Anal. Chem. 70:3946 (1998).
10. D. E. Stilwell and S.-M. Park, J. Electrochem. Soc. 135:2491 (1988).
11. E. K. W. Lai, P. D. Beattie, F. P. Orfino, E.Simon, and S. Holdcroft, Electrochim. Acta 44:2559 (1999).
12. J.-Y. Sung and H.-J. Huang, Anal. Chim. Acta 246:275 (1991).
13. S. Kuwabata, K. Mitsui, and H. Yoneyama, J. Electroanal. Chem. 281:97 (1990).
14. P. N. Bartlett and E. N. K. Wallace, Phys. Chem. Chem. Phys. 3:1491 (2001).
15. P. N. Bartlett and E. Simon, Phys. Chem. Chem. Phys. 2:2599 (2000).
16. D. E. Stillwell and S.-M. Park, J. Electrochem. Soc. 136:427 (1989).
17. S.-A. Chen and H.-T. Lee, Macromolecules 28:2858 (1995).
18. W. J. Albery, Electrode Kinetics, Oxford University Press, Oxford, 1975.
19. F. Zuo, R. P. M. Call, J. M. Ginder, M. G. Roc, J. M. Leng, A. J. Epstein, G. E. Asturias, S. P. Ermer, A. Ray, and A. G. MacDiamird, Synth. Met. 29:E445 (1989).
20. M. Angelopoulos, A. Ray, A. G. MacDiamird, and A. J. Epstein, Synth. Met. 21:21 (1987).
21. H. F. Mark and N. G. Gaylord, Encyclopedia of polymer science and technology, Interscience publishers, New York- London- Sydney, 1964.
22. N. Mano and A. Kuhn, J. Electroanal. Chem. 477:79 (1999).
23. N. Mano and A. Kuhn, J. Electroanal. Chem. 498:58 (2001).
24. L. L. Miller and J. R. Valentine, J. Amer. Chem. Soc. 110:3982 (1988).
25. M. F. Powell and T. C. Bruice, J. Amer. Chem. Soc. 105:7139 (1983).
26. R. E. Viola, P. F. Cook, and W. W. Cleland, Anal. Biochem. 96:334 (1979).
27. E. Katz, T. Lotzbeyer, D. D. Schlereth, W. Schuhmann, and H.-L. Schmidt, J. Electroanal. Chem. 373:189 (1994).
28. E. Katz, T. Lotzbeyer, D. D. Schlereth, W. Schuhmann, and H. L. Schmidt, J. Electroanal. Chem. 373:189 (1994).
29. N. Mano and A. Kuhn, Electrochem. Comm. 1:497 (1999).
30. C. X. Cai, L. H. Yin, and K. H. Xue, J. Mol. Cat. A, Chem. 152:179 (2000).
31. R. Braun, K. Santhanam, and P. Elving, J. Amer. Chem. Soc. 97:2591 (1975).
32. J. Moiroux and P. J. Elving, Anal. Chem. 50:1056 (1975).
33. J. Moiroux and P. J. Elving, J. Amer. Chem. Soc. 102:6533 (1980).
34. Z. Samec and P. J. Elving, J. Electroanal. Chem. 144:217 (1983).
35. P. J. Elving, W. T. Bresnahan, J. Moiroux, and Z. Samec, Bioelectrochem. Bioener. 9:365 (1982).
36. C. M. Halliwell, E. Simon, C. S. Toh, P. N. Bartlett, and A. E. G. Cass, Anal. Chim. Acta Accepted (2002).

37. C. M. Halliwell, G. M. Morgan, C. P. Ou, and A. E. G. Cass, Anal. Biochem. 295:257 (2001).
38. D. Matulis and R. Lovrien, Biophys. J. 74:422 (1998).
39. R. M. C. Dawson, D. C. Elliot, and K. M. Jones, Data for Biochemical Research, 1986.
40. B. W. Carlson and L. L. Miller, J. Amer. Chem. Soc. 107:479 (1985).
41. A. Brown and H. F. Fisher, J. Amer. Chem. Soc. 98:5682 (1976).